Quarterly Report

Project Title:
Development of a Self-Sustained Wireless Integrated Structural
Health Monitoring System for Highway Bridges

Cooperative Agreement # RITARS11HUMD

Fourth Quarterly Progress Report

Period:
April 15, 2012 through July 14, 2012

Submitted by:
The Research Team – University of Maryland with North
Carolina State University and URS

Submitted to:
Mr. Caesar Singh, Program Manager, US DOT

Date: October 25, 2012

Table of Contents

EXECUTIVE SUMMARY

I — TECHNICAL STATUS

Accomplishments by Milestone

1.1.   General
- Updated Project web site (http://www.ncrst.umd.edu/) (Task 1 and Deliverable 2)
- Delivered Forth quarterly financial and technical reports (Task 6 and Deliverable 11)
- Conducted several field meeting with NCDOT district engineer by Dr. Yuan (NCST) for selecting testing bridges and its logistics.
- MD Bridge No. 1504200 I-270 over Middlebrook Road, was first tested on March 19-21, 2012 during the University spring break. First draft was included in the Third quarterly report. Revised test report is included in this quarterly report as Appendix A.
- Second field test was conduct on June 28-29, 2012. Setup and initial results from the monitoring are covered in this report as Appendix B.
- Real time strain data monitoring is ready to view. (AE data is also ready to view.) The following web address should display the BDI strain data, both the graph and the properties.
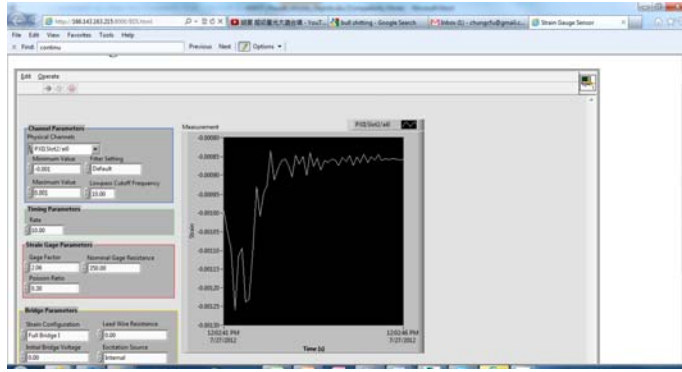 1) Try entering this web address into your browser (either Internet Explorer or Firefox should work fine)
  http://166.143.163.215:8000/BDI.html

  2) It will then ask you to download the Labview plug-in, and direct you to the webpage with the download.
  3) After the plug-in is downloaded and installed, you should be able to view the file.
  4) A captured real time strain is shown below.

- The proposed work plan is shown below as Milestones/Deliverables. Dark Shading indicates Deliverable items and Tasks in which the Research Team has been engaged over the past quarters. Lighter shading indicates anticipated duration for Deliverables by quarter.

Deliverables	Action	Quarter No.									
		1	2	3	4	5	6	7	8	9	10
1	Form TAC and conduct kick-off meeting. Determine baseline field test procedure (Task 1)	■									
2	Establish and update project web site (Tasks 1 & 6)	■	■	■	■	▦	▦	▦	▦		
3	Conduct baseline field test and finite element analysis on pre-selected bridges (Task 1)	■	■								
4	Design, fabricate and characterize AE sensor and measure the performance (Task 2)	■	■	■	■						
5	Develop and evaluate T-R method for passive damage interrogation (Task 3)	■	■	■	■						
6	Develop and experimentally evaluate wireless smart sensor and hybrid-mode energy harvester (Task 4)	■	■	■	■						
7	Implement passive damage interrogation T-R algorithm in the wireless smart sensor on bridges (Task 4)	■	■	■	■	▦	▦				
8	Integrate and validate AE sensors with wireless smart sensor and hybrid-mode energy harvester (Task 5)	■	■	■	■	▦	▦				
9	Develop and conduct field implementation/validation of commercial-ready ISHM system with remote sensing capability (Task 5)	■	■	■	■	▦	▦	▦			
10	Recommend strategy to incorporate remote sensing and prognosis into BMS (Task 5)	■	■	■		▦	▦	▦	▦		
11	Prepare and submit quarterly status and progress reports and final project report (Task 6)	■	■	■		▦	▦	▦	▦	▦	▦
12	Submit paper to conference presentations and publication to TRB meeting or other conferences (Task 6)	■	■	■		▦	▦	▦	▦	▦	▦

1.2. Remote Health Monitoring System
- Purchased AirLink Raven Gateway for wireless networking and 3G connection
  - Configured remote connection capabilities with the PXI
  - Activated Gateway with static IP address
- Purchased Aluminum Outdoor Casing
  - Case is equipped with fans for climate control
  - Drilled hole for sensor wires and power cords
- Setup a 5GB cloud drive from Amazon® to store data files
  - Data files can be retrieved from our labs, with quick download times
- Purchased a Kill-A-Watt®
  - Monitors power consumption of electrical devices
- Study the option using solar panel for sustainable system

1.3   Pilot Bridge Second Test
- MD Bridge No. 1504200 I-270 over Middlebrook Road testing was again performed on June 28-29, 2012, using deflection sensor for short term and AE and strain sensors for bridge long-term information collection. Stress range records were collected, which will be used as a reference for future testing. (Task 2 and Deliverables 4 & 9)
- Conducted full test of the second pilot bridge field test – Full test was conducted and its FEM analyses of this pilot bridges were conducted. Appendix B shows the complete report of MD Bridge No. 1504200. (Task 2 and Deliverables 4 & 9)
- Analyzed and organized detailed structural information of the Swing Bridge at Beaufort County by the NCST team. (Task 3 and Deliverable 5 & Task 4 and Deliverable 6)

1.4   AE Sensor
- Conduct long-term monitoring test on the I-270 bridge near Germantown, Maryland (see Figure 1)：seven piezoelectric film AE sensors including two piezo paint AE sensors were installed to monitor the growth of existing fatigue cracks on a connection plate (on Girder #3 of Southbound part) of the steel girder bridges. The sensors are connected to preamplifiers and PXI high speed data acquisition system for long term AE signal collection and fatigue crack monitoring. Also, to measure the differential deflection between adjacent girders (which is believed to the cause for fatigue cracks in connection plate of the girders), laser distance sensor was used to measure the differential deflection between Girders #2 and #3.

- Testing and validating piezo film AE sensor in the lab with more extensive tests to characterize its performance including on large scale structural test specimens - Major work conducted in this quarter includes (1) new design of piezo paint based acoustic emission (AE) sensors were fabricated by an external flexible circuit manufacturer – Tramont (order received in February) and sensor performance was examined in lab in March and April 2012; Additional 40-dB preamplifiers were made in our lab to accommodate these piezo film AE sensors both for lab and field tests. Calibration test involving glass capillary breakage and pencil break test (see Figure 2) were conducted to characterize the broadband performance of piezo film AE sensors. (2) Fatigue test frame and full-scale tube specimens were installed in our lab (see Figure 3). This test frame and specimens are currently used for full scale characterization of piezo paint based AE sensor; (3) Further experimental test of a frequency

shift based crack source location algorithm was conducted on the calibration setup shown in Figure 1 and other steel plates with a 1-in thickness. This near-field AE monitoring strategy is being refined for piezo film AE sensor and has the advantage of improved representation of crack source information. and (4) A Labview-based virtual instrument software for data acquisition of AE data was enhanced by adding new functionalities including automatic link to database and remote sensing ability.

(a) Installing piezo film AE sensors on connection plate

(b) installing PXI high speed data acquisition system
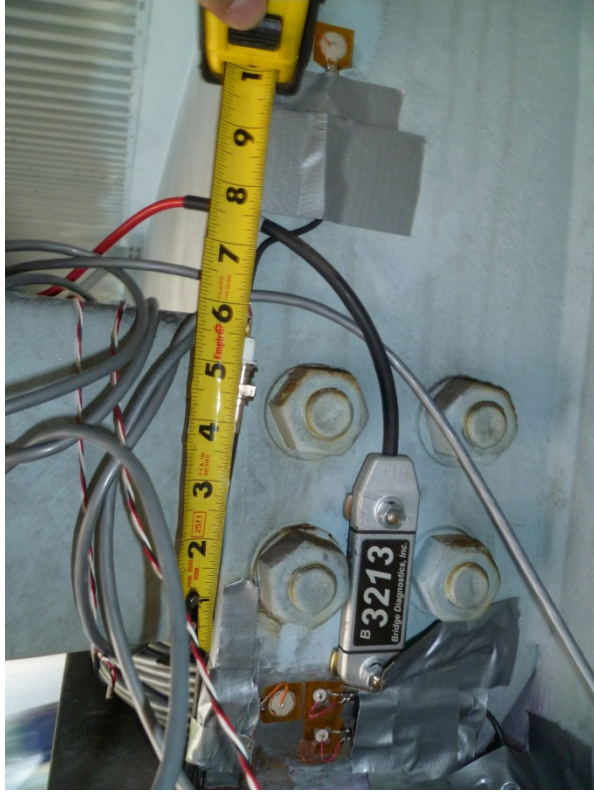
(c) piezo film AE sensors installed on connection plate

Figure 1. Pictures taken during field test on I-270 bridge in June 2012
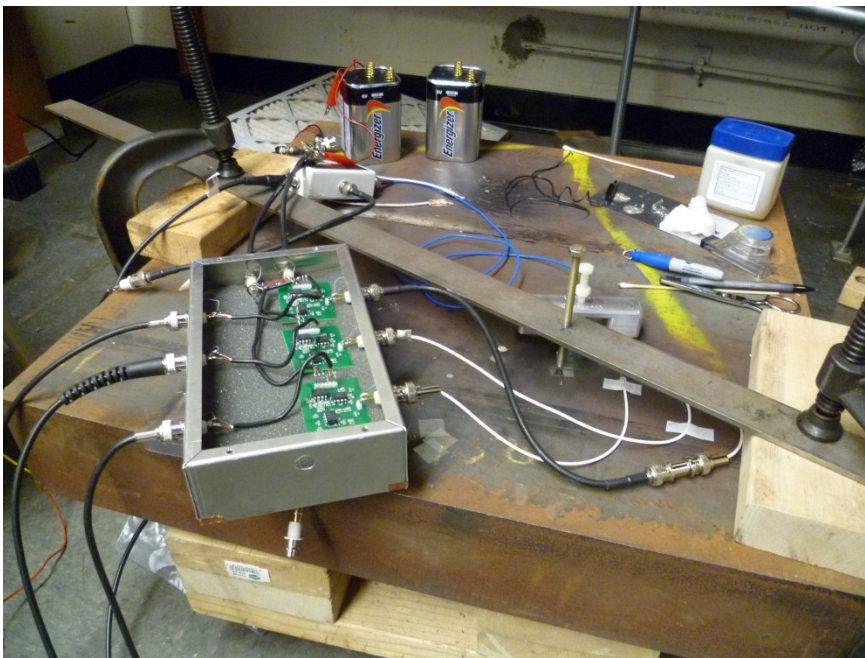
Figure 2. Calibration setup for piezo paint AE sensor

Figure 3. Fatigue test setup for full scale piezo paint sensor characterization test

1.5   T-R Method, Energy Harvesting and Smart Sensor

Accomplishments of these tasks are detailed in Appendix C and summarized here:
- Analyzed and organized detailed structural information of the Swing Bridge at Beaufort County Established the signal processing system (Task 3 and Deliverable 5 & Task 4 and Deliverable 6)
- The polysilicon solar power system for bridge health monitoring, which mainly consists of solar panel, miniature wind turbine, support and box, has been designed. (Task 4 and Deliverable 6)

- The output power of the selected solar panel has been calculated and tested. A Buck-Boost Converter has been designed and manufactured, and a rechargeable battery with a capacity of 5 amp hour was selected for storing the energy from the solar panel.. (Task 4 and Deliverable 6)
- A box in Fig. 8 with battery, Buck-Boost Converter, wireless transmitter and acceleration sensor has been manufactured, and it will be installed in the bridge. (Task 4 and Deliverable 6)

- Finish the design of a wireless accelerometer board. (Task 4 and Deliverable 6)

- Finish the design of a wireless accelerometer board. (Task 4 and Deliverable 6)
- Designed the communication protocol of the new wireless accelerometer board. (Task 4 and Deliverable 6)

1.6   Future Plans
Pilot Bridge Testing -
- Continue monitoring, evaluating and validating results from the 2nd pilot testing bridge (MD Bridge No. 1504200 I-270 over Middlebrook Road)
- Long-term monitoring using AE sensors on the pilot test bridge in Maryland
- Field testing T-R method, energy harvesting and smart sensors on the pilot test bridge in NC
- Simulating traffic through FEM models for all pilot test bridges in Maryland and NC
- Validating test data with FEM results

AE Sensor -
- Conduct long-term fatigue crack growth monitoring with piezo film AE sensor and remote sensing features on I-270 bridge in Maryland: in the last quarter, this long term monitoring system was installed and we have checked the system is working normally. In the next quarter, AE signals will be collected from this system and analyzed for possible fatigue crack growth associated with the existing fatigue cracking on the bridge.. Integrating wireless transmitter with piezo paint AE sensor is planned during the field test.
- Conduct testing AE sensor on full scale tube specimens in the lab - piezo paint AE sensor with new pattern to maximize frequency shift caused by fatigue crack growth will be tested in the steel welded tube specimens in lab. The next quarter will involve characterizing these AE sensors with integrated wireless sensing feature. The setup consists of a 5 ft long steel tube from traffic signal structure as shown in Figure 2. Eight piezo film AE sensors will be installed on each specimen to monitor any AE signal caused by fatigue crack initiation and propagation. The fatigue life is estimated to be 200k cycles under a stress range of 18 ksi, which is comparable to the stress level observed on the connection plate of the field test bridge in Maryland.
- More differential girder deflection using laser distance sensor will be conducted.

T-R Method, Energy Harvesting and Smart Sensor -
- Manufacture the miniature wind turbine and its Buck-Boost Converter.
- Finish the communication protocol of the wireless accelerometer board. Test all the wireless accelerometer sensors in the Lab.
- Install the wireless sensing system on the bridge

II — BUSINESS STATUS

- Hours/Effort Expended – As the last reporting period, PI Dr. Fu worked one month paid by his cost sharing account for 167 man-hours. Three (3) UM and two (2) NCSU graduate assistants worked three months half-time (20 hours), the quarterly accounting deadline, for a total of 1,470 man-hours (one NCSU assistant is partially cost-shared by their University.)
- Hours/Effort spent by the MD State for in-kind cost share ($125,000) is counted for here. Hours/Effort by the NCDOT for in-kind cost share will be counted for in the next quarter.
- Funds Expended and Cost Share –
  o Listed and invoiced in this Quarterly Federal Financial Report (period ending on June 30, 2012): Federal share of expenditure requested for this quarter $101,901.03 [Federal share total $316,292.08; Recipient share of expenditure (cost share) $244,606.10, which is shown in an excel file; Cumulative Total $560,898.18]
  o $125,000 in-kind cost sharing contribution by MDSHA on equipment, personnel, consultation, and road-side assistance on the March 26-28 bridge test is included.
  o Cash contribution includes $97,996.69 by UMD and $21,609.41 by NCSU.

Appendix A –   **Updated UMD Report for MD Bridge No. 1504200 I-270 over Middlebrook Road**

Appendix B – **Remote Strain Measurement at the Crack Location for MD Bridge**

Appendix C -   **NCST Report for NC Structure No. 060025 Swing Bridge at Beaufort County**

Appendix A - Updated Field Test Report for Bridge No. 1504200 I-270 over Middlebrook Road
By
Dr. Chung C. Fu, PE, and Dr. Yunfeng Zhang

Field test dates: March 19 to 21, 2012
Bridge Type: Single-span composite steel I-girder bridge (span length = 140 ft.; Figure 1)
Location: I-270 (Southbound) over Middlebrook Road near Germantown, Maryland (Figure 2)
Participants:

    UMD Dr. Fu's group: Dr. Chung C. Fu; Graduate Students: Tim Saad and Time Brinner (BDI strain transducer and Cable-Extension Transducer, or called string pot)
    UMD Dr. Zhang's group: Dr. Yunfeng Zhang; Graduate Students: Changjiang Zhou (AE sensor), Linjia Bai (wireless sensor), Zhen Li (laser distance sensor), and Feng Shi (ultrasonic distance sensor)
    URS Dr. Ed Y. Zhou (coordination and oversight)

Figure 1. View of the bridge
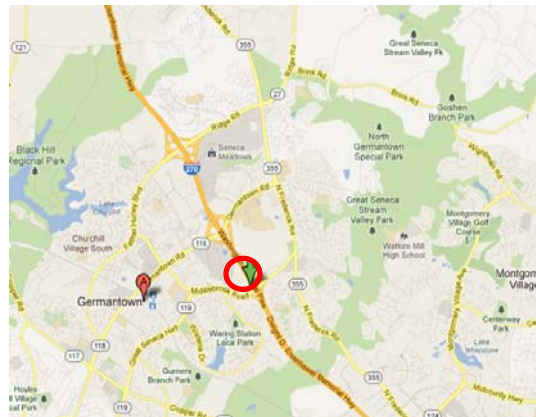
Figure 2. Bridge location (red circle, latitude=39.175296, longitude= -77.247046)

PHASE I – INSTRUMENTATION PLAN

The main data acquisistion (DAQ) systems used in this test are:

    a. PXI-based data acquisition system by National Instruments for data collection from BDI strain transducers, string pots and AE sensors
    b. Multi-channel data acquisition equipment CR5000 manufactured by Campbell Scientific, Inc. for extra BDI strain transducers

Types of sensors used in this project are: 1. piezoelectric paint AE sensors; 2. wireless accelerometers; 3. laser sensor; 4. ultrasonic distance sensors; 5. BDI strain transducers; and 6. String pots.
Instrumentation plan is shown in Figure 3 – Crack locations and sensor placement on the framing plan.
Also shown are Figures 4-7 for cracks on Girders 3 & 4 and their respective sensor locations.

Figure 3 – Crack locations and sensor placement on the framing plan
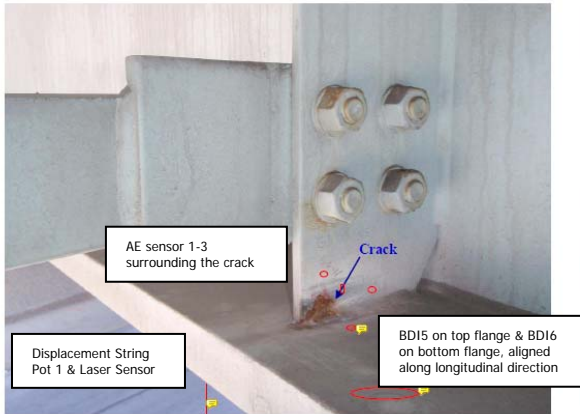
Figure 4. Crack at G3B2D3 (Girder 3 Bay 2 Diaphragm 3) and sensor

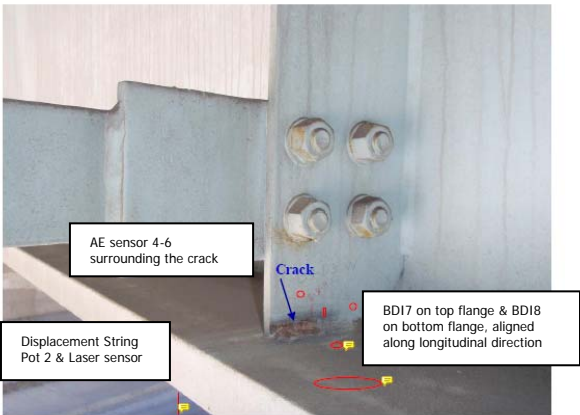Figure 5. No Sign of Cracking at G3B3D3 (Girder 3 Bay 3 Diaphragm 3) and one

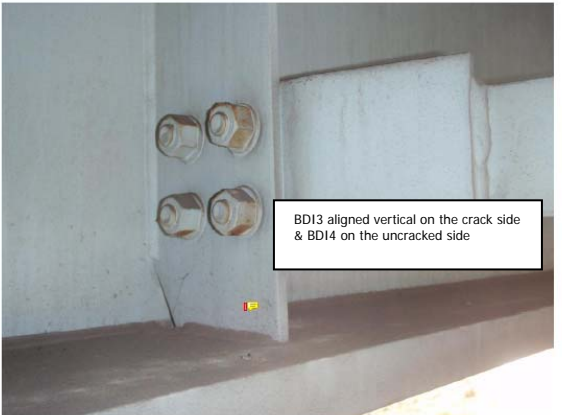Figure 6. Crack at G4B3D3 (Girder 4 Bay 3 Diaphragm 3) and sensor locations

Figure 7. No Sign of Cracking at G4B4D3 (Girder 3 Bay 4 Diaphragm 3) and one sensor

PHASE II – FIELD TEST AND RESULTS

1.   Acoustic Emission Monitoring

A total of seven AE sensors were installed on Girder 3 and Girder 4. Three piezoelectric paint AE sensors were installed on Girder 4. Two of them were placed on the cracked connection plate (see Figure 8) while the third was placed on the uncracked connection plate to provide ambient noise AE data (Figure 9). Figure 10 shows the installation of those AE sensors. Same arrangement is for Girder 3.
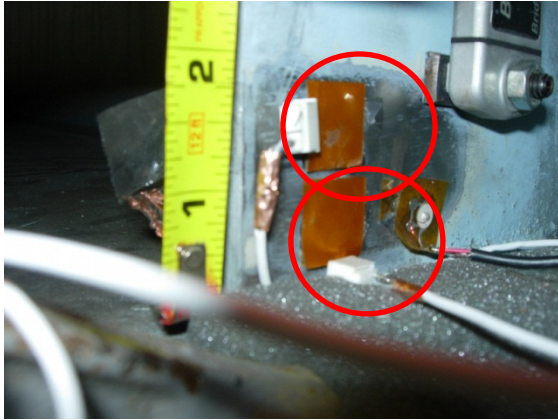
Figure 8. Piezoelectric paint AE sensor on cracked connection plate (red circled, for monitoring fatigue crack in the weld between the connection plate and lower

Figure 9. Piezoelectric paint AE sensor (blue circled, for monitoring ambient noise since there is no fatigue crack on this side connection plate)

(a)

(b)
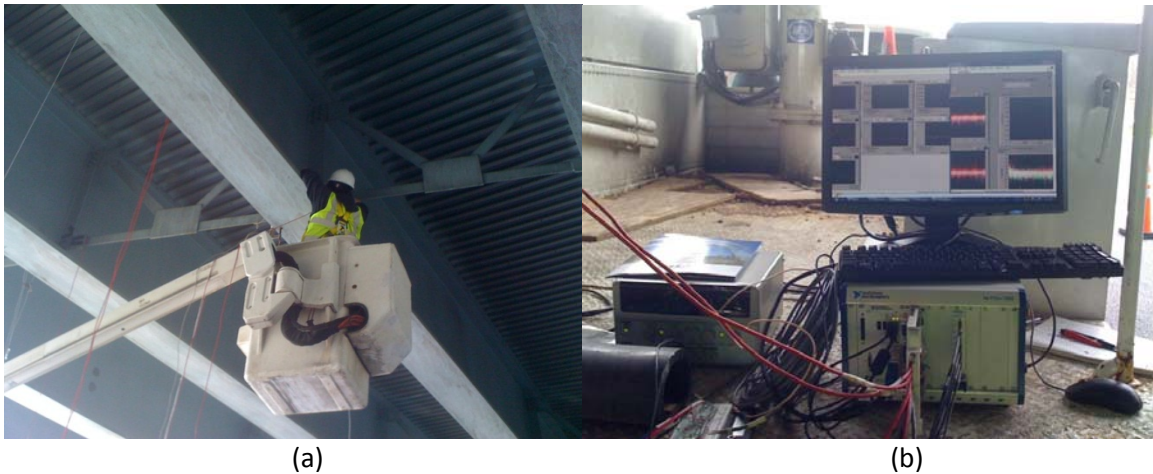
Figure 10. (a) Installing AE sensors and wiring; (b) AE data acquisition

Installing AE sensors and wiring took quite some time on March 20 and 21, 2012. The first day (March 19) of field test was spent on surface preparation for installing AE sensors and preparing additional preamplifiers for AE sensors. The second day (March 20) was on installing AE sensors and connecting wires and preamplifier for three AE sensors. During the third day (March 21), most of the time was spent on wire connection and debugging the sensors. Data were collected from all seven AE sensors. Continuous AE monitoring was carried out from approximately 1:10pm to 1:55pm on March 21, 2012. Based on past bridge monitoring experience with piezo paint AE sensor and on-site trial on AE data collection, the trigger threshold was set to be 50 mV for each AE sensor channel over this monitoring period (otherwise, if a lower threshold level is used, overly large AE data sets would be collected with much significant AE events), that is, if the AE signal for each chancel exceeds 50 mV, data collection would be triggered and a total of 10,000 data points (5 msec.) will be collected for each channel at a sampling rate of 2 MHz. Over this monitoring period, no fatigue-crack-related AE signal is observed. Samples of AE data and their frequency characteristics (by applying FFT on time series data) are shown in Figure 11. This is probably due to the short AE monitoring period (only 45 minutes) during this field test during which perhaps no heavy loaded trucks crossed the bridge. It is recommended that for the

next field test, a longer monitoring period (e.g., at least three consecutive days) be arranged to collect AE signals related to fatigue crack growth.
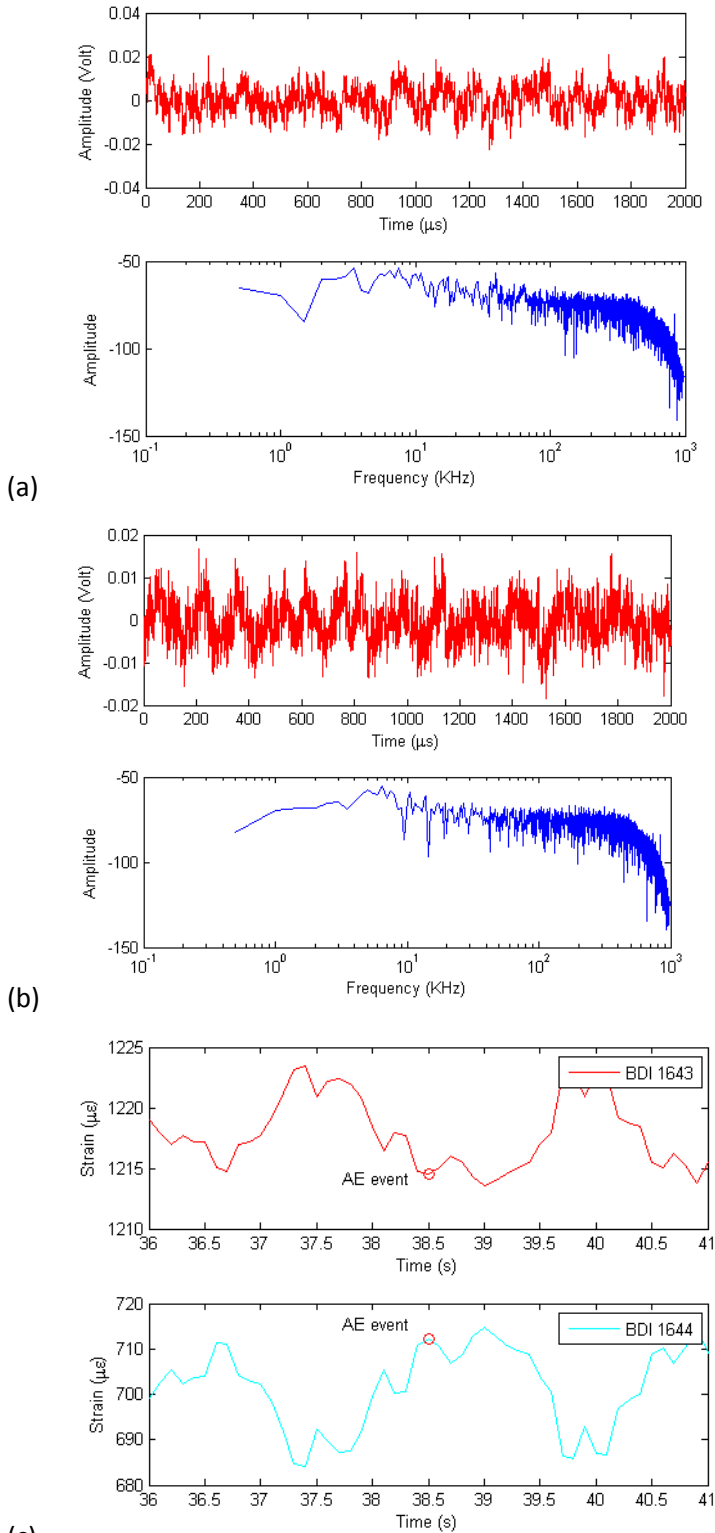

(a)

(b)

(c)

Figure 11. AE data collected by piezo paint AE sensor on Girder 4: (a) ch4 AE data on cracked connection plate; (b) ch6 AE data on uncracked connection plate ; (c) corresponding strain data

14

(from BDI strain gage near ch4 AE sensor), AE data acquired between 38.6 and 38.7 seconds in this figure (highlighted with red circles) (BDI 1643 strain gage on the uncracked side of Girder 4 while BDI 1644 strain gage placed on the cracked side of Girder 4).

2. Wireless Sensor (monitoring vibration responses of Girders 2 to 5 of the bridge)

A total of four wireless accelerometers (see Figure 12) Imote2 were used to monitor the vibration responses of the bridge. One wireless sensor was installed on one of the girders (Girder 2 to 5) and acceleration data was acquired at 100 Hz sampling rate synchronically. The acceleration data was used to provide modal frequency information (Figure 13) that can be used to calibrate the finite element model of the bridge. The fundamental frequency thus measured is 3.22 Hz, which is very close to the value from finite element analysis (3.14 Hz).

Figure 12. Wireless sensor Imote2 (measuring acceleration and temperature)
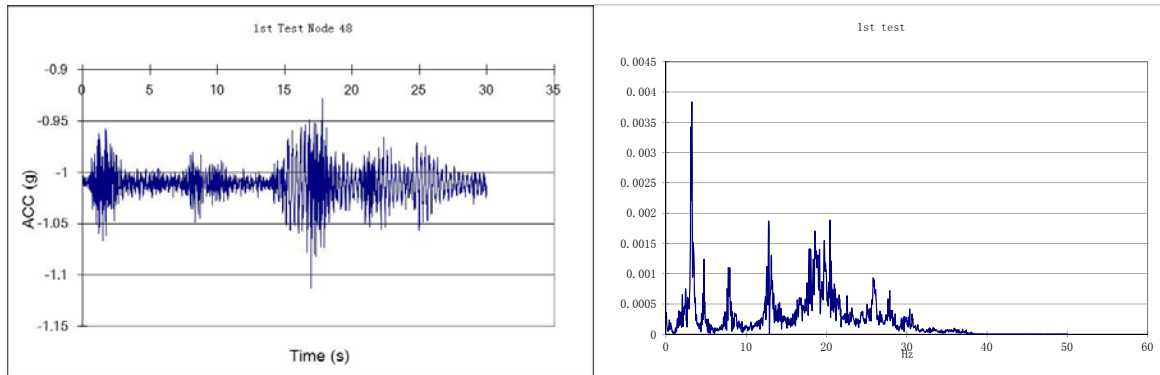
(a) Acceleration time history

(b) FFT of acceleration data (horizontal axis: frequency; vertical axis: FFT amplitude)

Figure 13. Acceleration data measured by wireless sensor

3. Bridge Deflection Monitoring

Both laser sensor and ultrasonic distance sensors were used to measure the dynamic deflection of the bridge, as shown in Figure 14. Only one laser sensor and one ultrasonic distance sensor were used each

time. The data from laser sensor is shown in Figure 15. The measured deflection value from the laser sensor agrees well with the string pot, and its accuracy is also validated by the fundamental frequency indicated by FFT of the laser sensor measured deflection data (see Figure 16). The ultrasonic sensor data had some problems, most likely due to a high sampling rate (20 Hz seems to be too high for ultrasonic distance sensor of this particular model, next time we will lower the sampling rate to 5 Hz, which provides much better accuracy during lab calibration test) and parasitic echo signals from reflecting background such as lower surface of bridge deck (next field test we will install the ultrasonic distance sensor on the girder and let it shoot down on road surface to avoid background noise).

Table 1. Maximum deflection measured by laser sensor

Girder #	3	4	5
MaxD (m)	0.0066	0.0069	0.0063

Note: MaxD=average(Distance)-minimum(Distance)
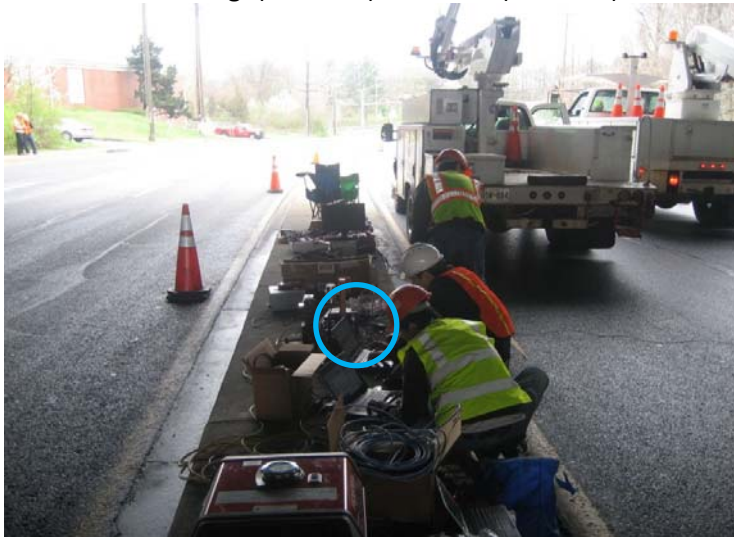
Figure 14. Bridge deflection measurement with ultrasonic distance sensor and laser distance sensor (in blue circle)
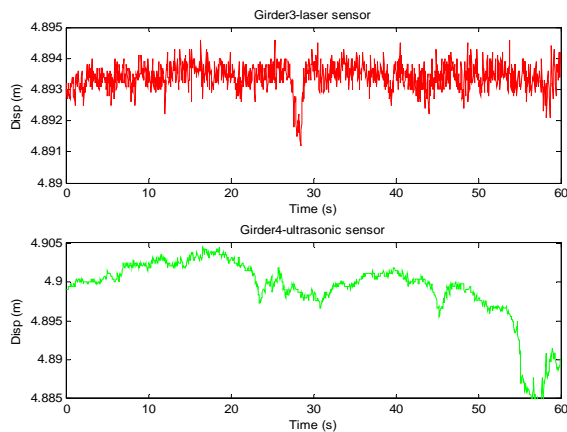
Figure 15. Bridge deflection data by laser sensor (upper) and ultrasonic sensor (lower)
(The measured value is the distance between the sensor and girder bottom surface)
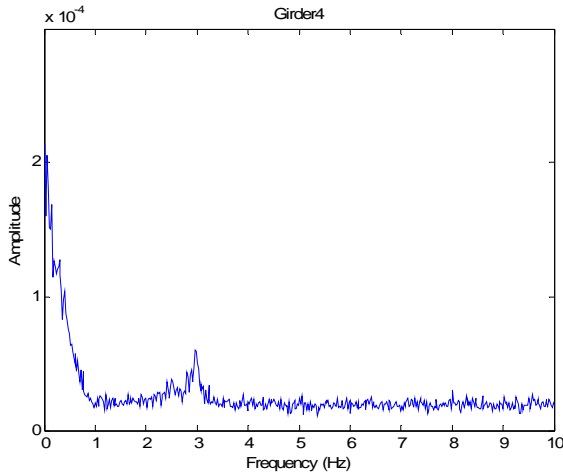
Figure 16. FFT of laser distance sensor
(note the existence of fundamental frequency of the bridge near 3 Hz)

4. BDI Strain Transducers

BDI 1-4 strain transducers were placed on both sides of the connection plates while BDI 5-8 were placed on the top and bottom flanges on Girders 3 and 4 (Figures 4-7). Since each transducer is unique and individually calibrated, their numbers are marked on Figure 17 for identification. Figures 18 and 19 are showing the measured live load stresses on the flanges and connection plates, respectively.

The maximum longitudinal stress measured on the bottom flange is 1.604 ksi in tension from BDI 3215 on the bottom flange of Girder 3. As for the connection plates, the maximum vertical stresses are 16.18 ksi in tension from BDI 1641 on Girder 3 and 16.1 ksi in tension from BDI 1644 on Girder 4.
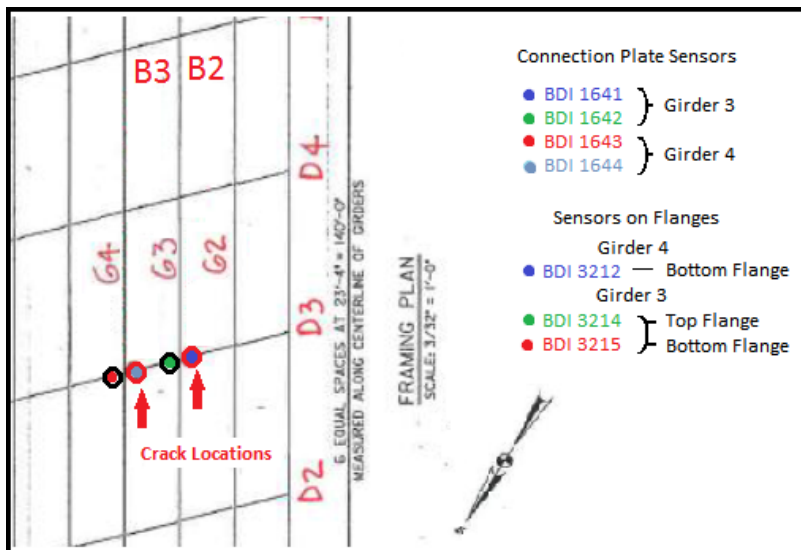
Figure 17. BDI strain transducer locations and marked numbers

17
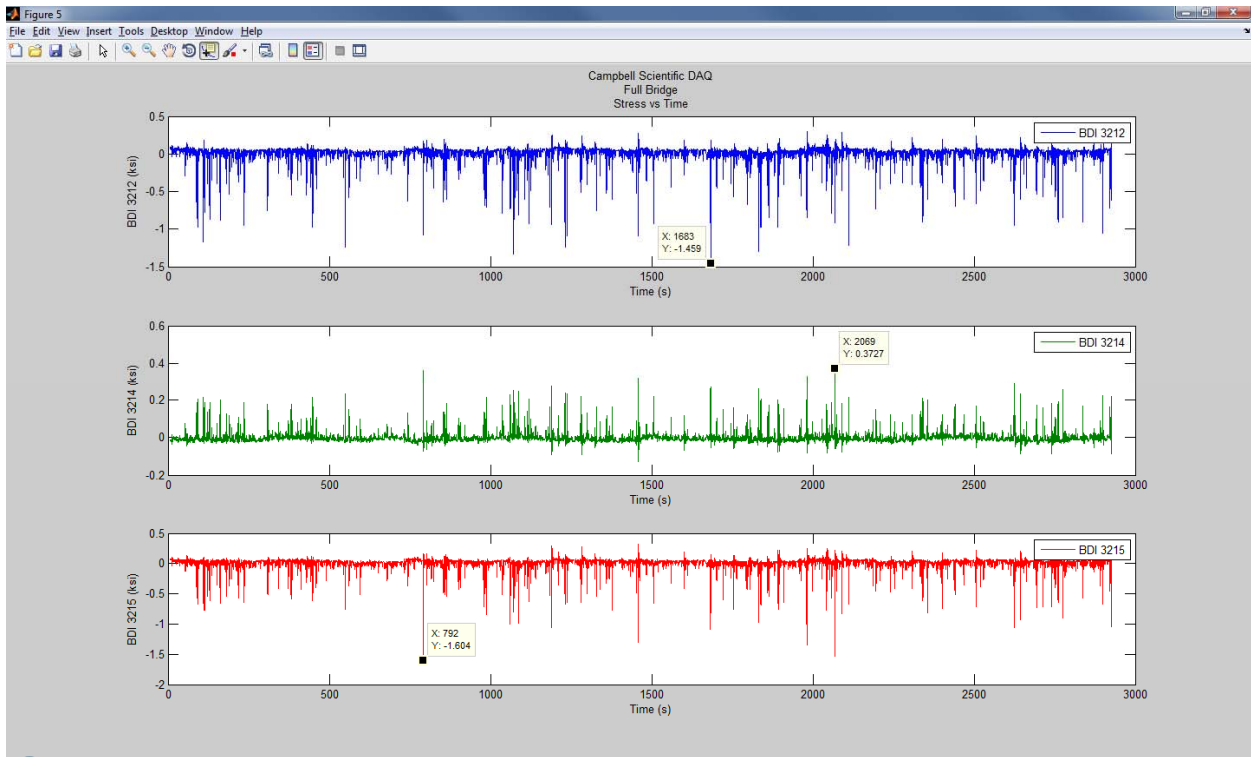
Figure 18. BDI strain transducer flange measurements on Girders 3 and 4
(Positive indicates tension; 3212 G4 bottom flange; 3214 G3 top flange and 3215 G3 bottom flange)
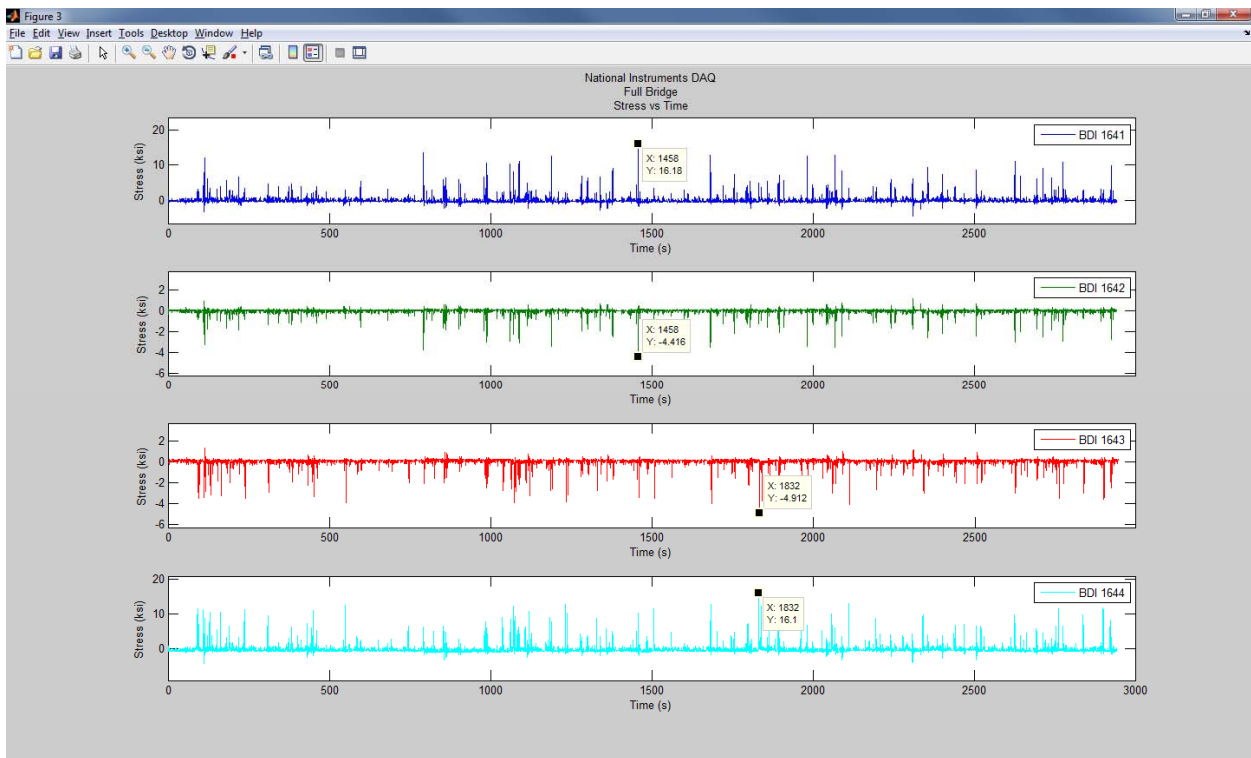
Figure 19. BDI strain transducer connection plate measurements
(Positive indicates tension; 1641 G3 cracked side; 1642 G3 uncracked side, 1643 G4 uncracked side and 1644 G4 cracked side)

5.   String Pots

String pots were placed on Girders 3 and 4, synchronized with strain and acoustic emission results. The maximum measurements within the testing period are 0.231" on girder 3 and 0.205" on girder 4, respectively, which are very closed to the laser results, though laser was independently measured. (This short-term measurement is lower than previously measure up to 0.5" or 0.75".)
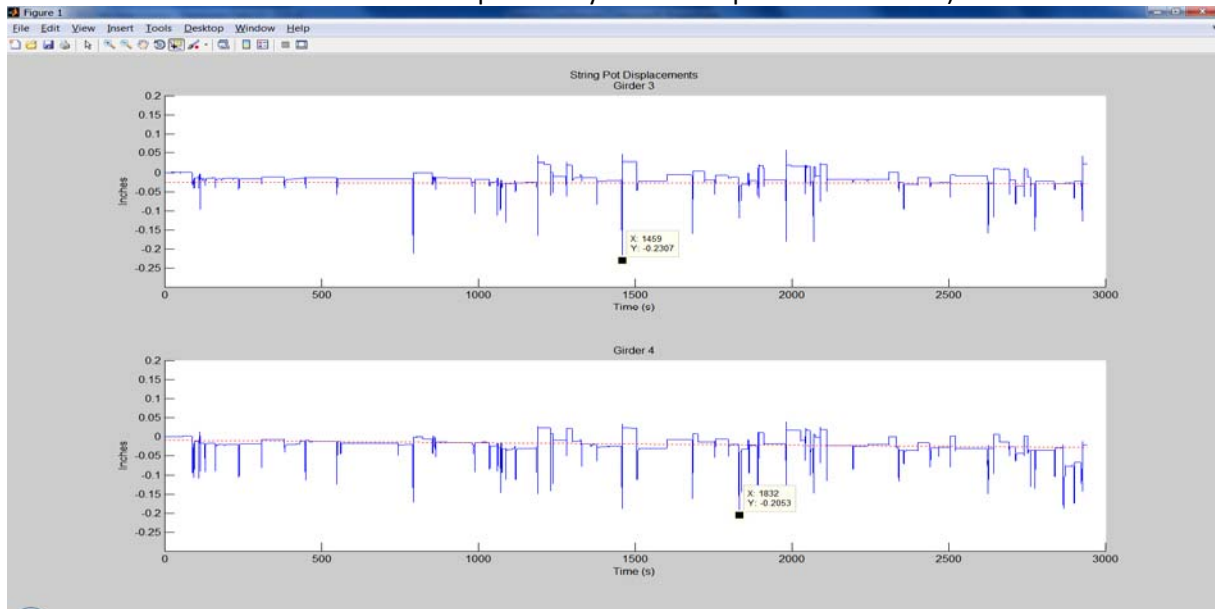
Figure 20. String pot deflection results on girders 3 and 4

PHASE III – FEM ANALYSIS

Finite element model was generated for the bridge. Its model is shown in Figure 21 and its first natural frequency is calculated around 3.11 for a fixed-fixed boundary condition and lower for the normal analysis of fixed-free boundary condition. This is a skewed bridge and the x-translational direction is along the longitudinal direction of the bridge. Fixed-fixed boundary condition represents all x-, y- and z-translational degrees-of-freedom of the five nodes at the bottom flange for each girder on both ends are fixed while fixed-free boundary condition represents x-translational degree-of-freedom of one end is freed (as a roller end). For comparing the first mode, fixed-fixed condition is more realistic where the test result is 3.22 Hz and FEM result for fixed-fixed condition is 3.14 Hz (Table 2).

19
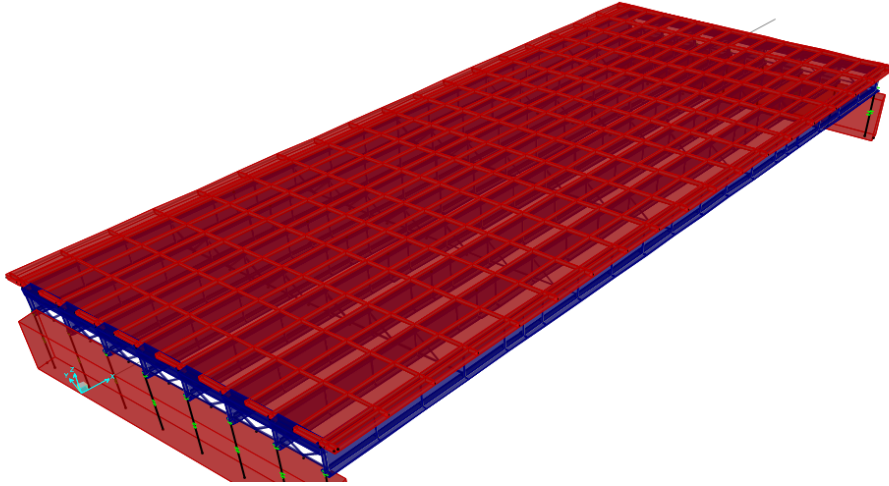
Figure 21. FEM model of the Middlebrook Road Southbound Bridge by CSI Bridge
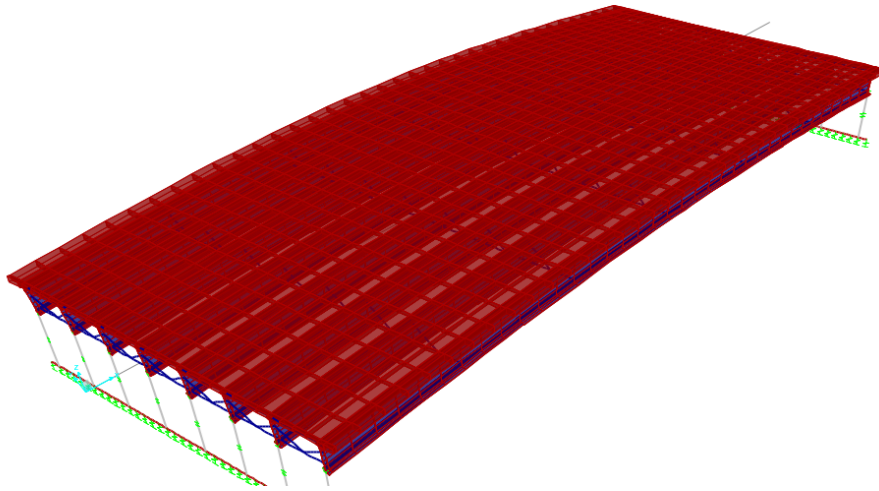
Figure 22. Modal shape of the first mode (f = 3.136 Hz) by CSI Bridge

Table 2 – Natural frequencies by FEM analysis

Hz	Fixed-Fixed	Fixed-Free
1	3.136131	2.235395
2	3.204958	2.730252
3	5.483081	5.030165
4	5.581643	5.16084
5	6.518478	6.48045

To simulate the traffic, Weigh-in-Motion data was collected from the Hyattstown southbound station, which is located on I270 about 10 miles north of the tested bridge. A more accurate simulation process is still under development. In order to get approximate traffic loading, seven cases of HS-20 truck loading with run stream on different lanes of different patterns were simulated which are:

Case 1: 3 trucks passed the bridge one by one (one at a time) in different lanes

Case 2: the 3rd truck entered the bridge when the 1st truck just left the bridge (only two trucks on the bridge at the same time)
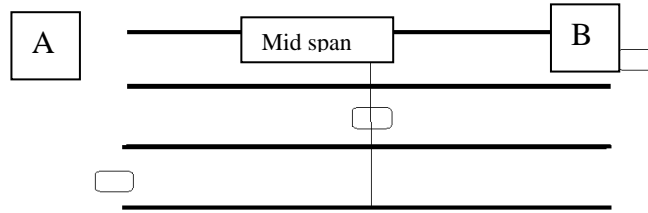
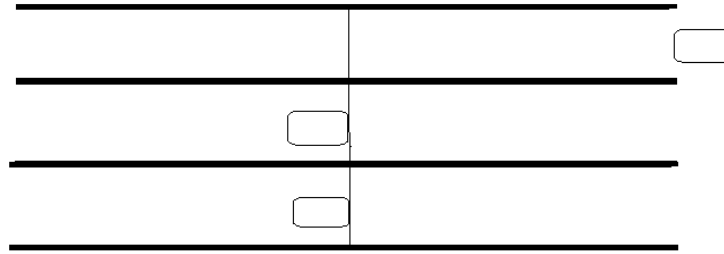Case 3: the 3rd truck entered the bridge when the 1st truck and 2nd truck just left mid span
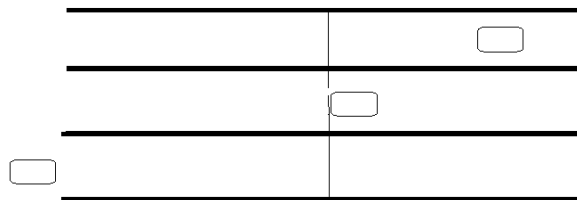
Case 4: the 1st truck left the bridge when the 2nd truck and 3rd truck just entered the right span one after the other
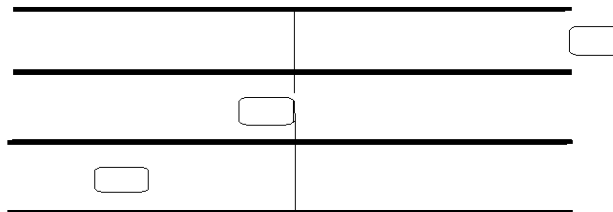
Case 5: the 1st truck and the 2nd truck passed the bridge parallel
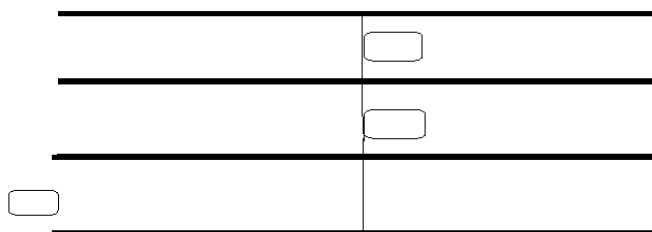
Case 6: the 1st truck just left when the 2nd & 3rd truck is @ mid span

Case 7: 3 trucks passed the bridge at the same time, no truck load reduction is applied
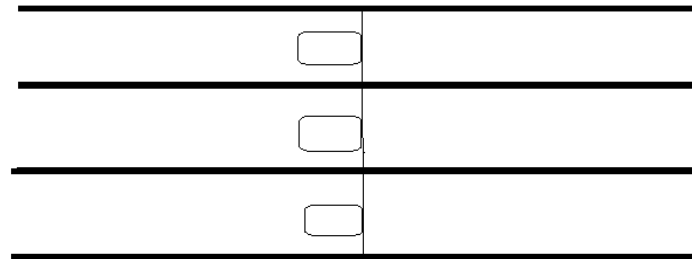
Table 3 – Maximum bottom flange stress ranges of seven truck simulation cases

	GIRDER3	GIRDER4
LL_CASE	ksi	ksi
CASE1	1.229	1.281
CASE2	1.249	1.343
CASE3	1.239	1.281
CASE4	1.507	1.486
CASE5	1.189	1.316
CASE6	1.926	2.128
CASE7	2.245	2.369

Since this is a simple-span bridge, the maximum stress ranges at the bottom flange are close to the maximum stresses, which are demonstrated in Figure 18. The maximum stress measured on the bottom flange of girder 3 is 1.604 ksi where the FEM maximum stress ranges for case 4 for two HS-20 loaded subsequently on two near lanes is 1.507 ksi and case 6 for two HS-20 loaded on two near lanes is 1.926 ksi, respectively. Case 7 for three lane lsimultaneously loaded, based on AASHTO LRFD Specifications that can be reduced by a multiple presence factor of 0.85, yields 1.908 ksi (0.85*2.245 ksi). Global tress contour and its close-up view (in kips/ft^2; divided by 144 to convert the scale to ksi) are shown in Figure 23 (a) and (b). Due to program limitation, the connection plates were not modeled.
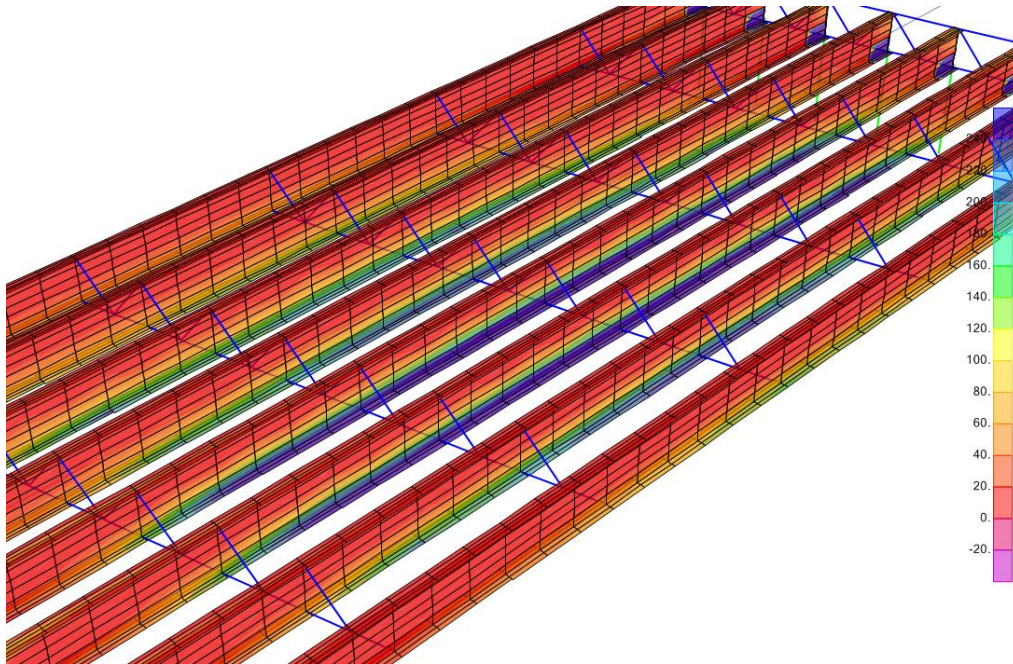
(a) Global stress contour (in kips/ft^2) of eight southbound girders (looking south)
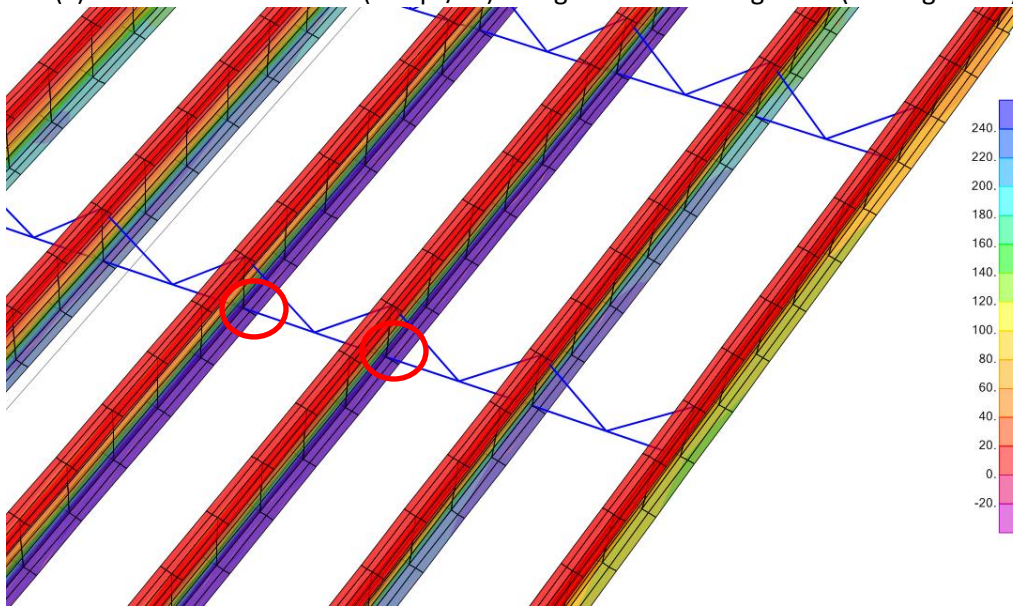
(b) Close-up view of girders 3 and 4 with fatigue cracks

Figure 23. Live load stress contour of truck loading case 6

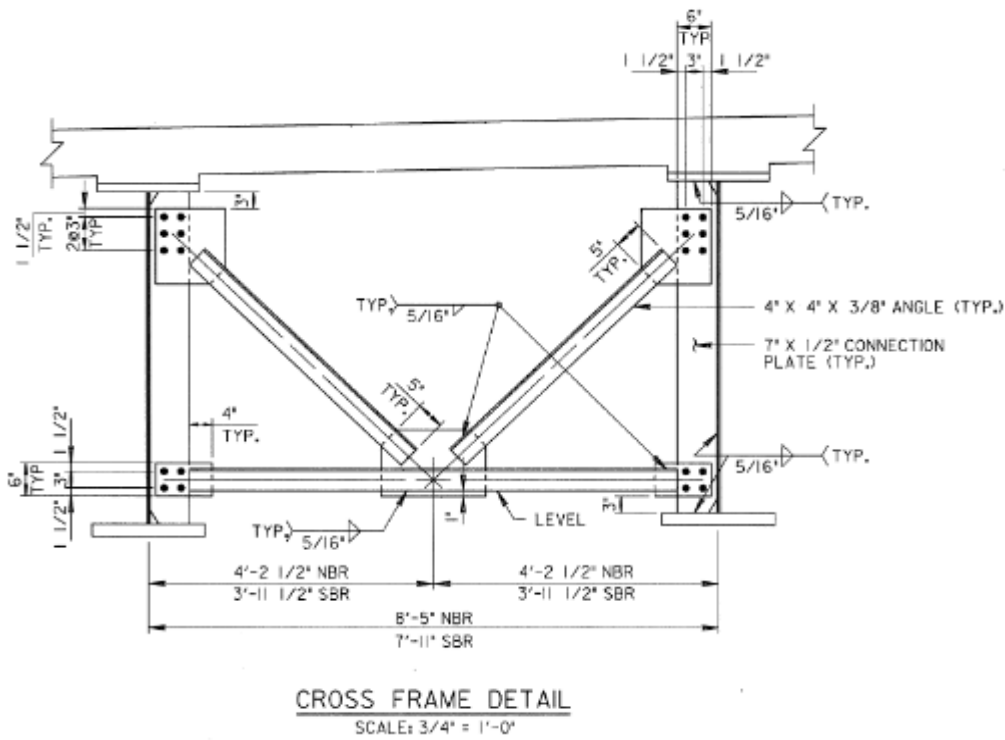**High tension stress on the connection plates on Girders 3 and 4**

Figure 24. Typical cross frame detail

Out of all types of cross-frames, X-type with top and bottom chords is the stiffest of all, then the K-type with top and bottom chords, then the X-type with bottom only and the flexible one is the K-type with bottom chord only. Differential displacement between girders will cause one diagonal in tension and one in compression. Since the working point of the diagonal is not at the junction of girder web and top flange plus no help from the top chord, one side of the connection plate will be under tension and one under compression. Measured 16.1 ksi in tension is not surprising with the flexibility of the cross-frame and the girder system (with up to 0.5" to 0.75" vertical deflections due to live load observed.)

Figure 25 shows the numbering for the cross-frames near the crack locations.   Table shows their corresponding forces.
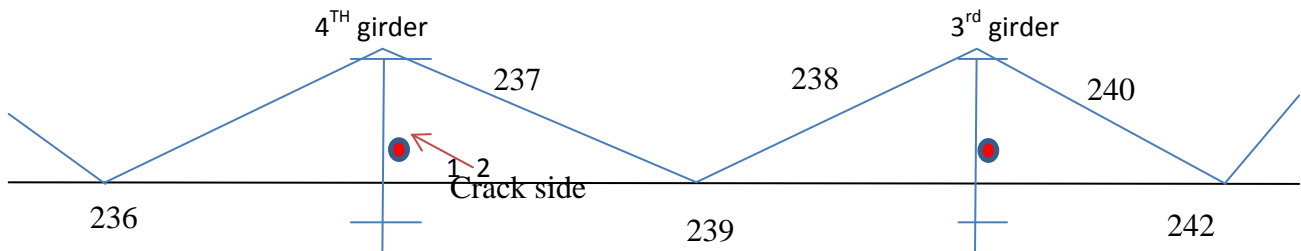
Figure 25. FEM numbering for the cross-frames near the crack locations

Table 4. Cross-frame maximum envelop element forces of seven simulated live load cases

24

Max. Envelop		P (kip) for #236		P (kip) for #239		P (kip) for #242	
	Element	Tension	Comp	Tension	Comp	Tension	Comp
CAES1_LL	1	13.37	-0.94	15.42	-0.23	13.58	-1.37
	2	15.39	-0.23	13.56	-1.41	8.33	-1.18
CASE2_LL	1	13.55	-0.45	16.14	-0.13	14.32	-1.30
	2	16.10	-0.14	14.28	-1.30	8.61	-1.15
CASE3_LL	1	10.69	-0.85	6.21	-0.24	13.69	-1.43
	2	6.24	-0.26	13.66	-1.45	8.33	-1.27
CASE4_LL	1	20.35	-0.88	17.42	-0.21	13.66	-0.26
	2	17.41	-0.23	13.64	-0.28	8.36	-0.23
CASE5_LL	1	22.19	-0.95	16.79	-0.15	14.58	-0.15
	2	16.74	-0.17	14.56	-0.17	8.39	-0.18
CASE6_LL	1	13.39	-0.13	21.23	-0.17	19.70	-1.14
	2	21.23	-0.17	19.63	-1.16	9.13	-1.06
CASE7_LL	1	21.36	-0.22	21.58	-0.26	18.16	-0.30
	2	21.56	-0.26	18.09	-0.31	8.08	-0.18

	P (kip) for #237		P (kip) for #238		P (kip) for #240	
	Tension	Comp	Tension	Comp	Tension	Comp
CAES1_LL	5.756	-6.606	6.612	-5.741	0.174	-3.62
CASE2_LL	5.524	-6.815	6.816	-5.507	0.106	-3.933
CASE3_LL	5.589	-2.65	2.649	-5.574	0.162	-3.696
CASE4_LL	5.731	-8.317	8.323	-5.712	0.163	-3.648
CASE5_LL	5.686	-8.125	8.136	-5.676	0.083	-4.269
CASE6_LL	0.1	-2.391	2.402	-0.101	0.085	-7.468
CASE7_LL	0.076	-3.008	3.028	-0.083	0.101	-6.957

In order to maximize the differential displacement and bracing elements, two more loading cases to simulate more truck traffics and field measured stresses are added to the run:

Case 16: the 1st group trucks passed the bridge side-by-side on fast lanes and 2nd group 25' behind
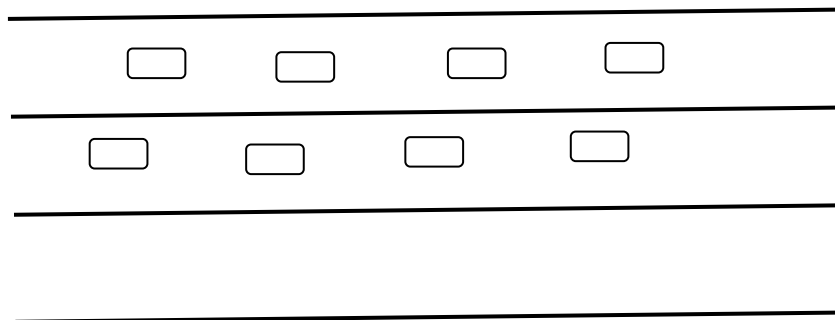
Case 17: the 1st group trucks passed the bridge side-by-side on slow lanes and 2nd group 25' behind
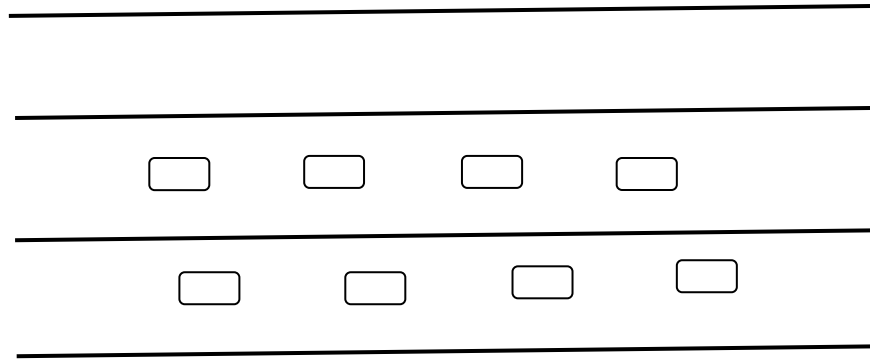
Max. stress	girder 3 crack location connected with the bottom chord between girder 2 and 3	girder 4 crack location connected with the bottom chord between girder 3 and 4
case 16_LL	**7.32ksi**	**17.95ksi**
case 17_LL	19.59ksi	21.68ksi

Maximum differential displacement of -0.316584 inches is found between girders 2 and 3 under live load case 16 (-0.303624 inches between girders 3 and 4).

Appendix B - Remote Strain Measurement at the Crack Location for MD Bridge
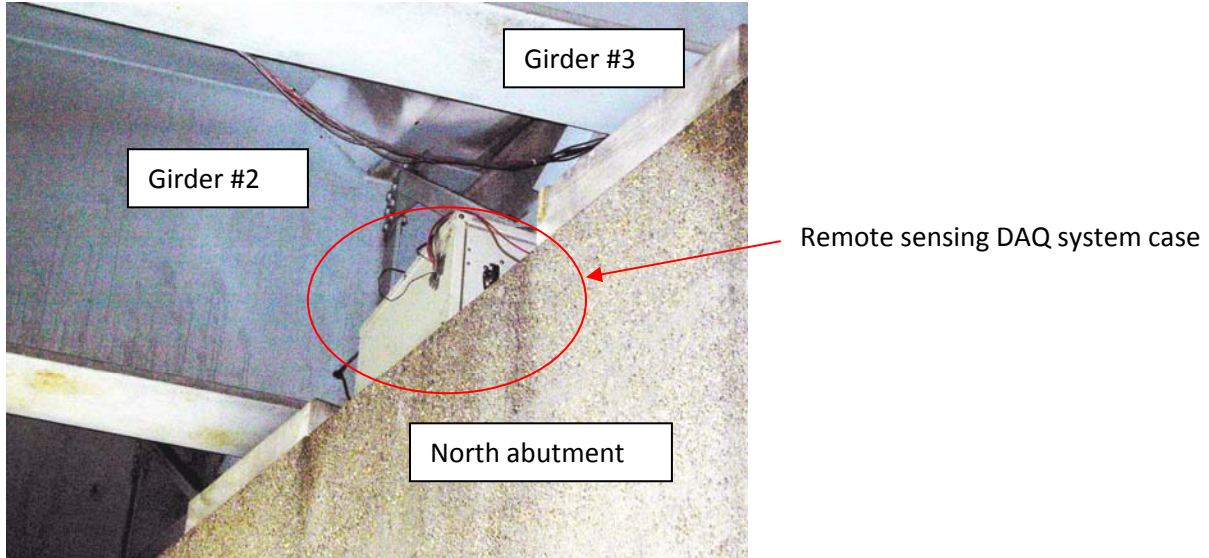
Figure 1 – Case containing remote sensing DAQ system on the top of the bridge pier
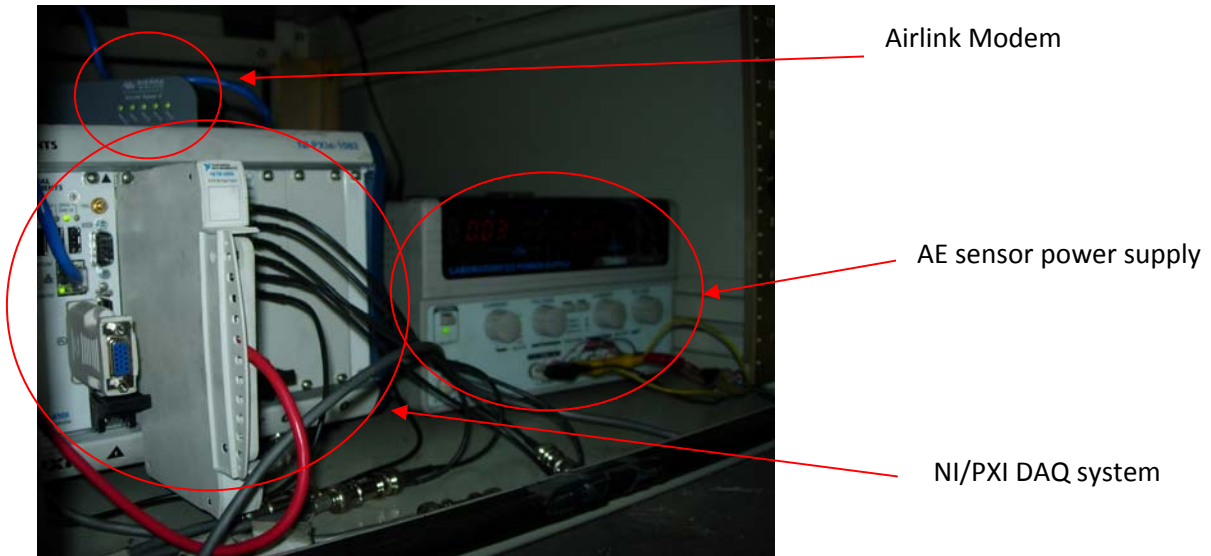
Figure 2 – Close look of the remote sensing DAQ system inside the case
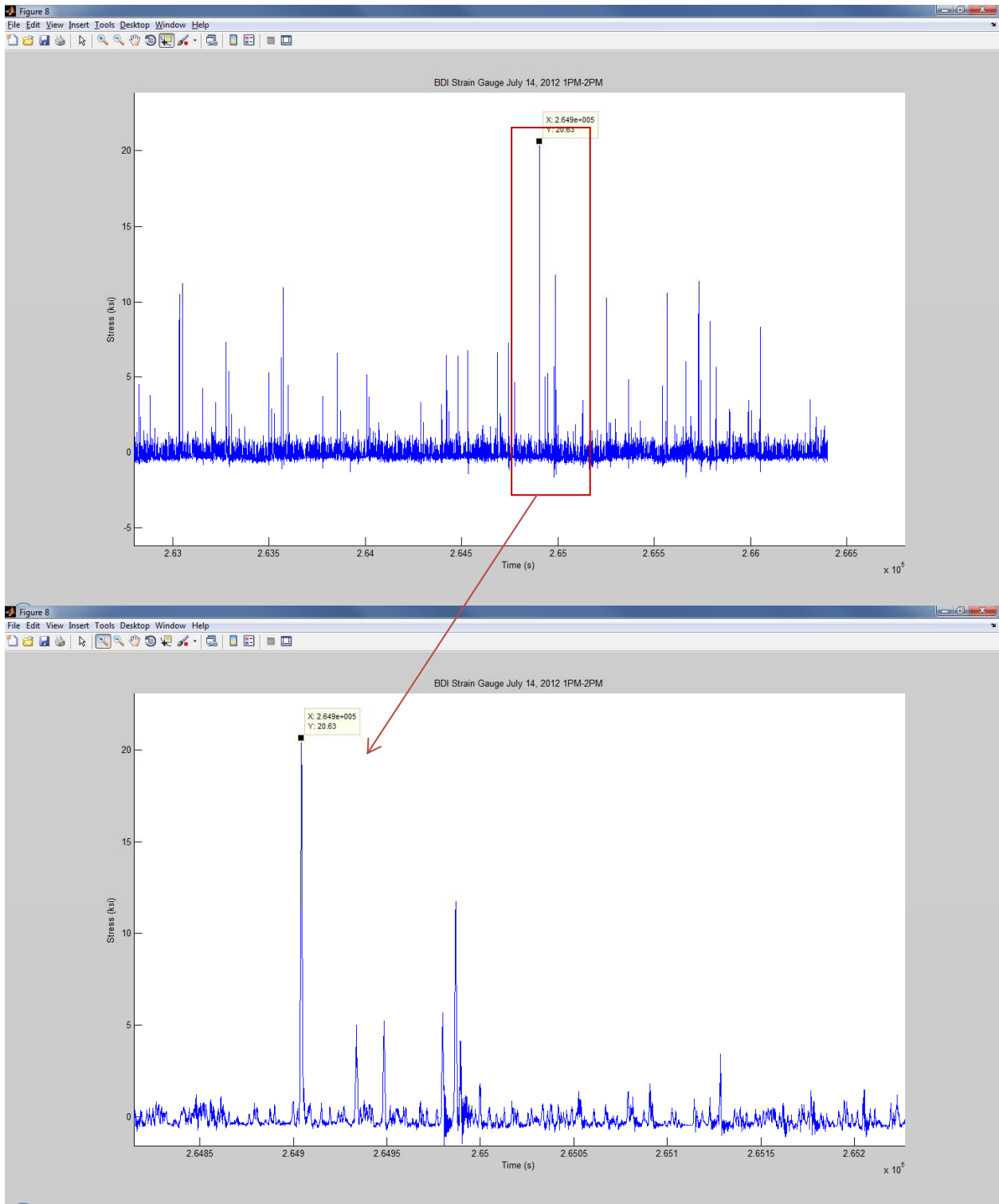
Figure 3 – Sample segment 1 of the continuously monitored strain data
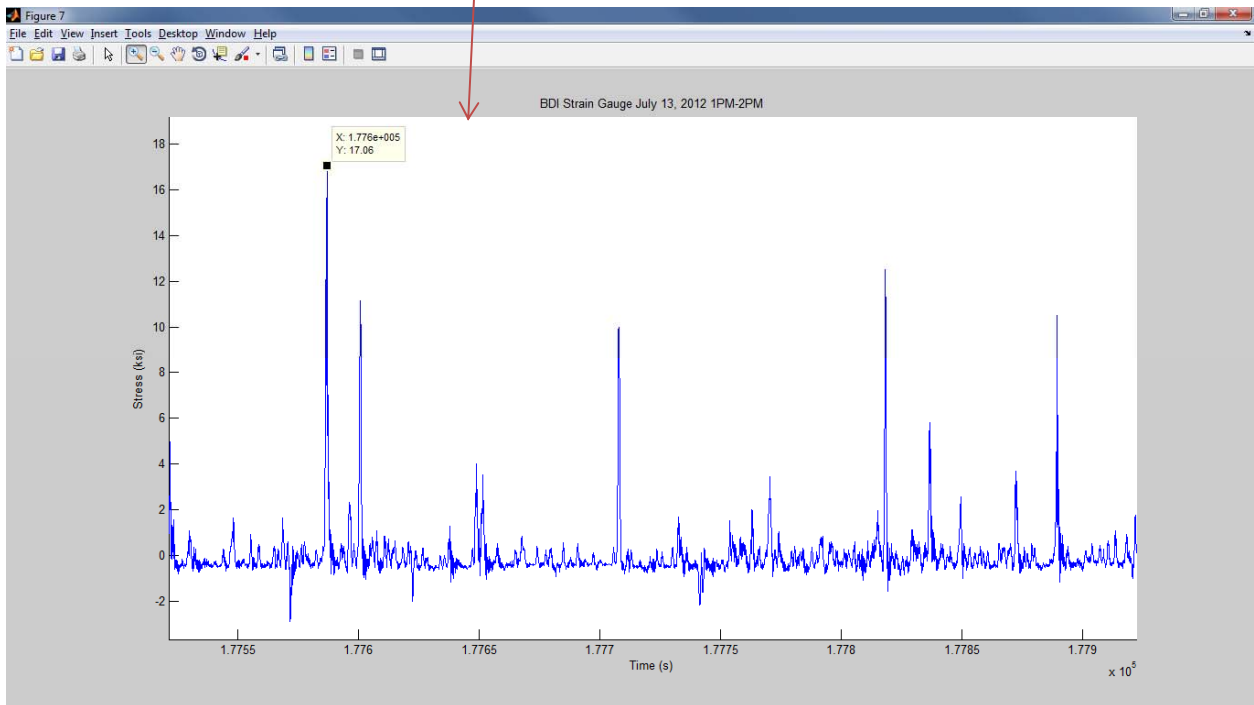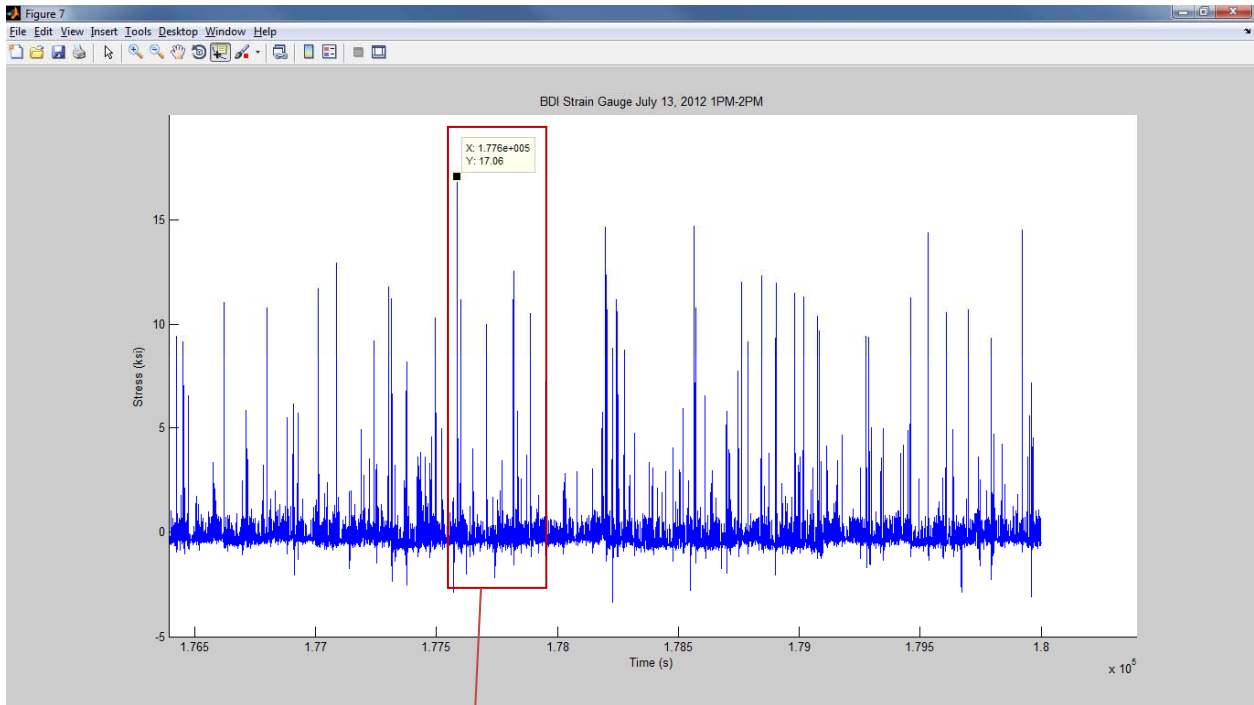
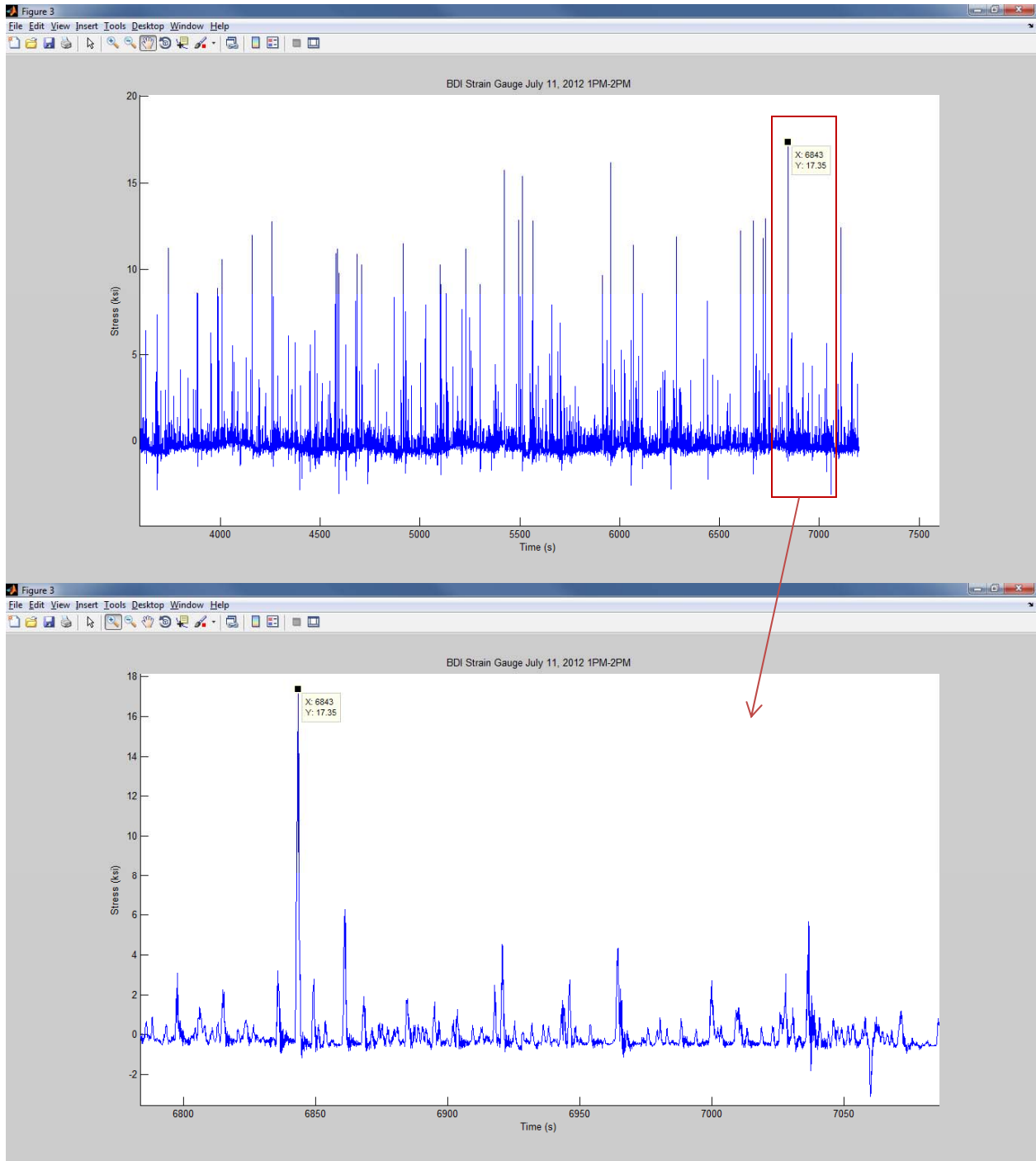Figure 4 – Sample segment 2 of the continuously monitored strain data

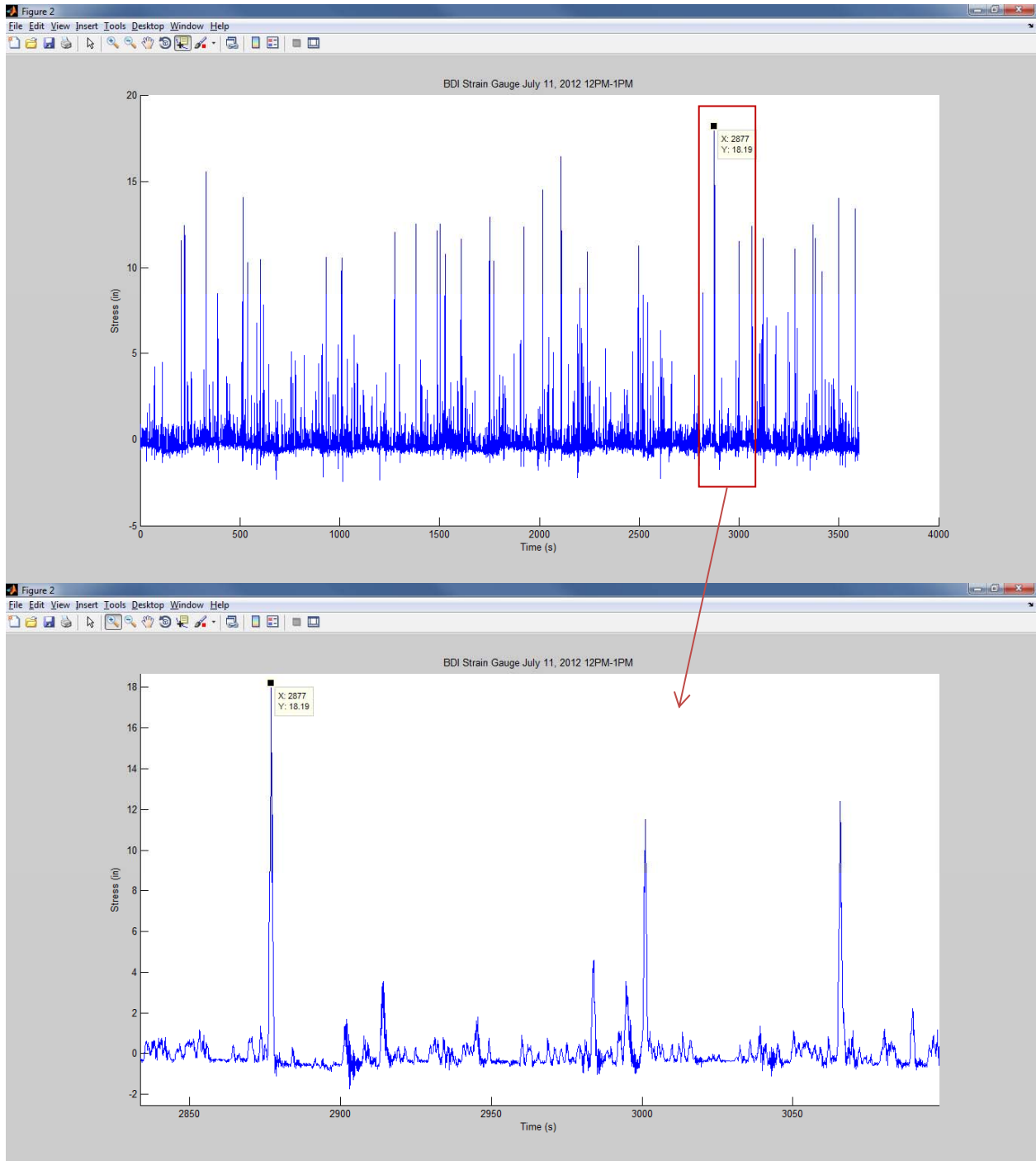Figure 5 – Sample segment 3 of the continuously monitored strain data

Figure 6 – Sample segment 4 of the continuously monitored strain data

Appendix C - NCST Detailed Technical Report

1-TECHNICAL STATUS
Accomplishments by milestone

- Established the signal processing system
  There are three aspects in this part: signal collection, signal transmission and signal processing. Fig. 1 is the overview diagram of the signal processing for the structural health monitoring system by wireless sensors.
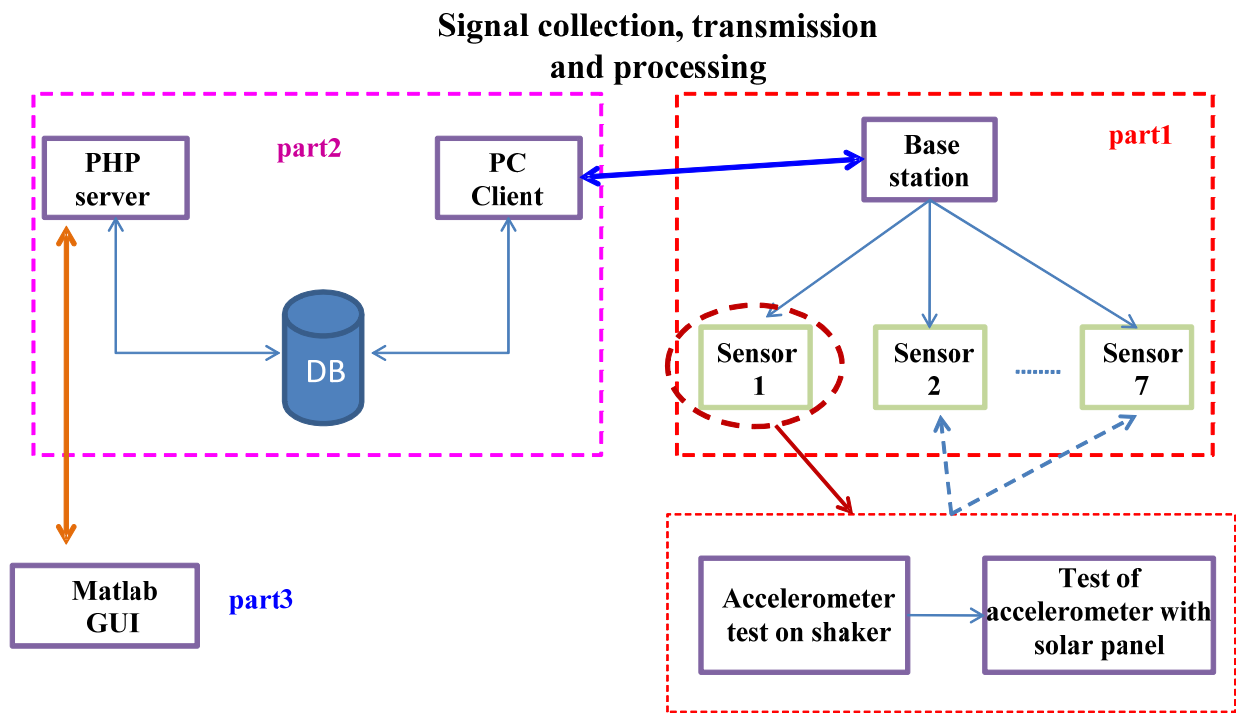

Fig. 1 overview diagram of signal processing

Signal collection is an important part of the signal processing which can collect information about the bridge structure by using the wireless sensors. The work has been done in this part includes: Seven wireless sensors are manufactured, the accelerometers in the sensors are tested, the program between wireless sensor and base station is compiled.

In the part of signal transmission, the signals collected by the sensors will be uploaded to our server or website by using the internet, and the server or website would provide the download service, that is to say, we can get signal from the server or website. The following link is our website about our work: http://leibaobao.com/dot/msViewNetwork.php. Fig. 2 is the website we built on the internet, and Fig. 3 is the base station which we can use it to upload the

signals. The work has been done in this part includes: the base station has been built, the website has been built, the program between base station and server is compiling.
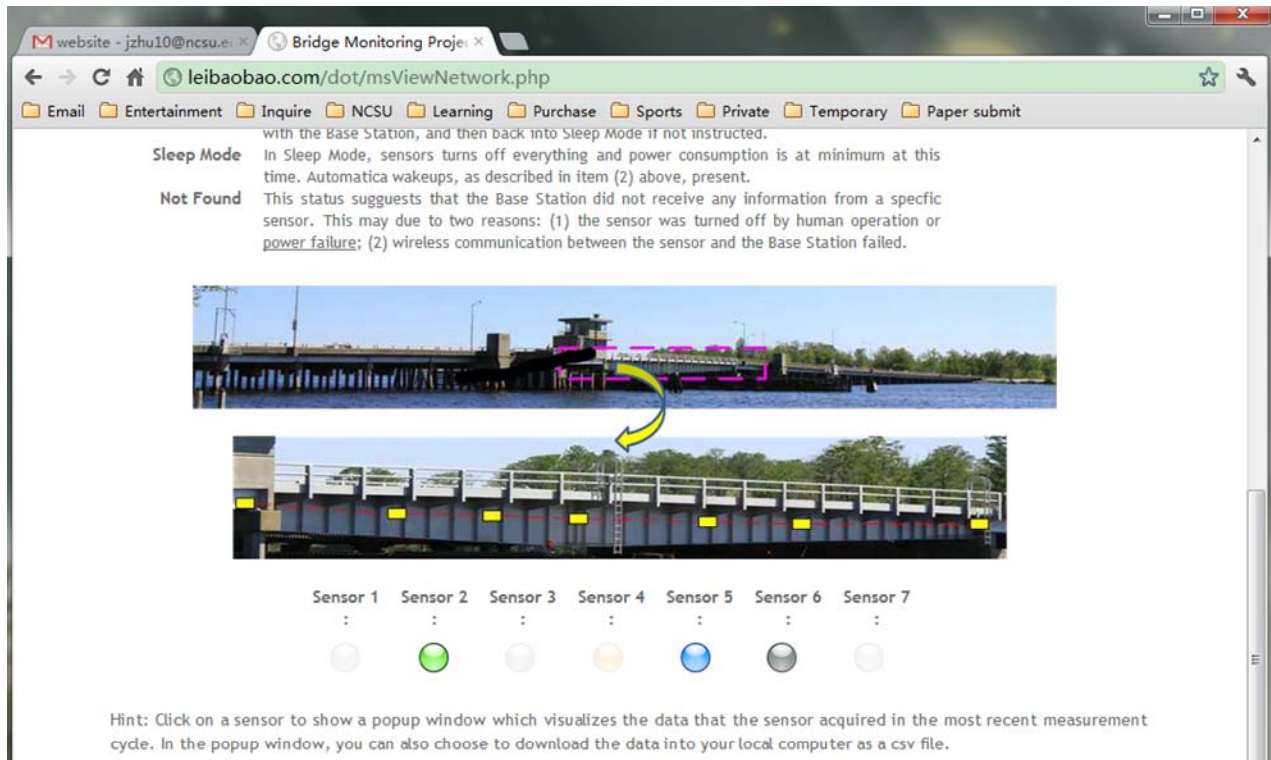

Fig. 2 The website for structural health monitoring system

Fig. 3 the base station for transmitting signals

The signals will be processed and displayed in the signal processing part. So we built the GUI to dispose the signal which can be downloaded from the server or website. Fig. 4 is the GUI panel, which can be divided into three parts: communication, signal display and modal shape. Fig. 5 is the panel to display how to obtain the signals from the communication part.
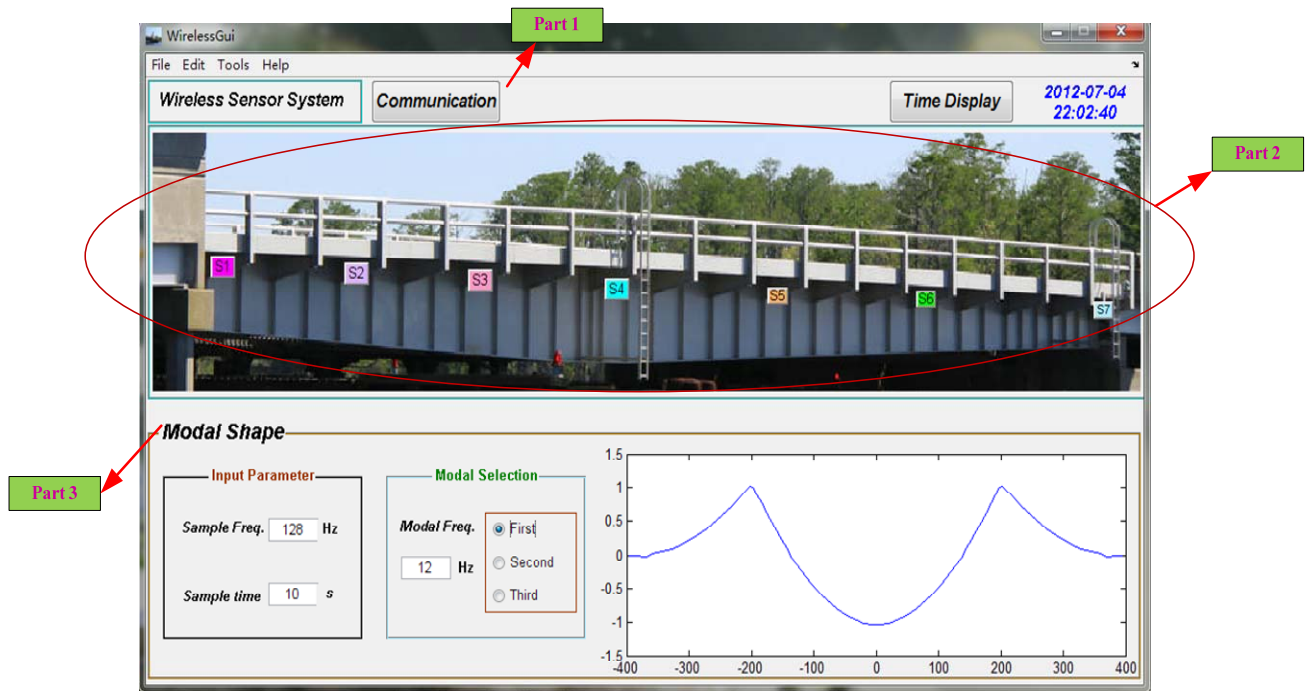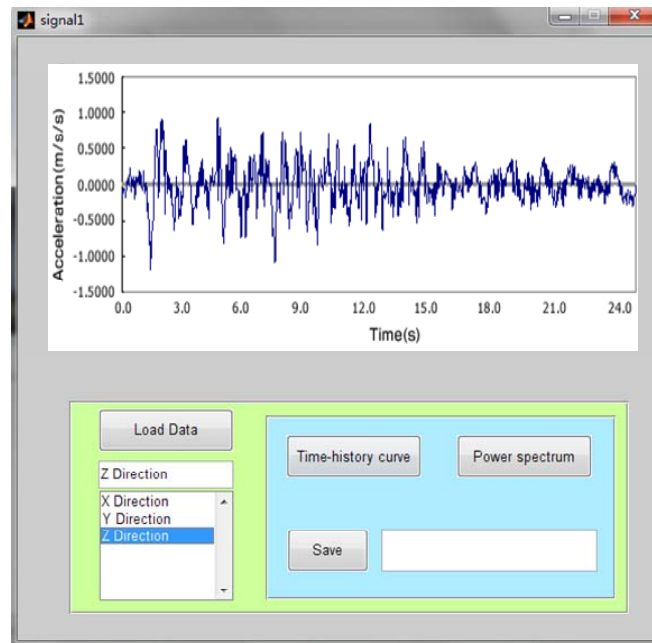
Fig. 4 GUI panel

Fig. 5 Signal display panel

- The polysilicon solar power system for bridge health monitoring, which mainly consists of solar panel, miniature wind turbine, support and box, has been designed, as shown in Fig. 6.
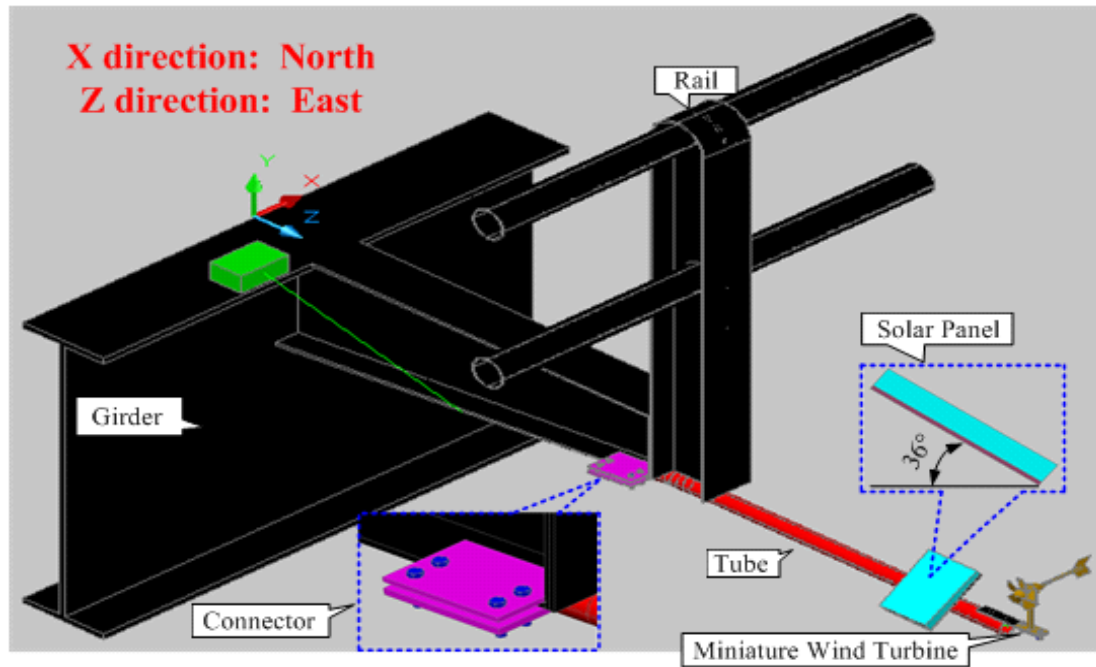

Fig. 6 Polysilicon solar power system

- The output power of the selected solar panel has been calculated and tested. A Buck-Boost Converter (Fig. 7) has been designed and manufactured, and a rechargeable battery with a capacity of 5 amp hour was selected for storing the energy from the solar panel. The effectiveness of the Buck-Boost Converter has been experimentally verified. The calculated output power of the solar panel can be seen in Table 1, the tested output power of the solar panel and efficiency of the Buck-Boost Converter can be seen in Table 2.

Table 1 Calculated monthly average daily output power of the solar panel (Wh)

Jan.	Feb.	Mar.	Apr.	May	June	July	Aug.	Sept.	Oct.	Nov.	Dec.
8.93	7.85	9.45	10.84	10.51	9.59	10.72	11.03	10.31	7.79	9.12	7.30

Table 2 Tested values of the solar panel and Buck-Boost Converter

Date and time	Parameters	Values
(2012-5-24) 9:30-17:30	Daily Output Current (mAh)	1459.4
	Daily Output Power (mWh)	9861
	Daily Input Current (mAh)	2322
	Daily Input Power (mWh)	8869

Efficiency of the circuit	0.899
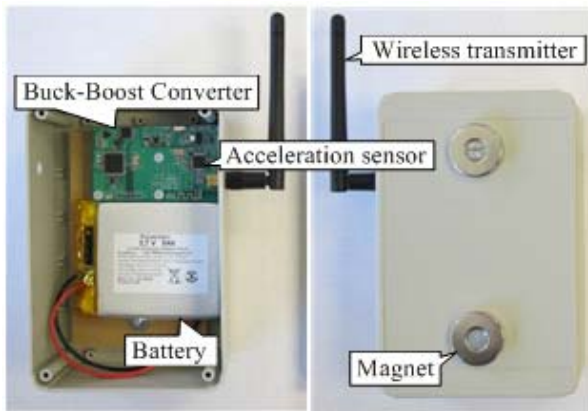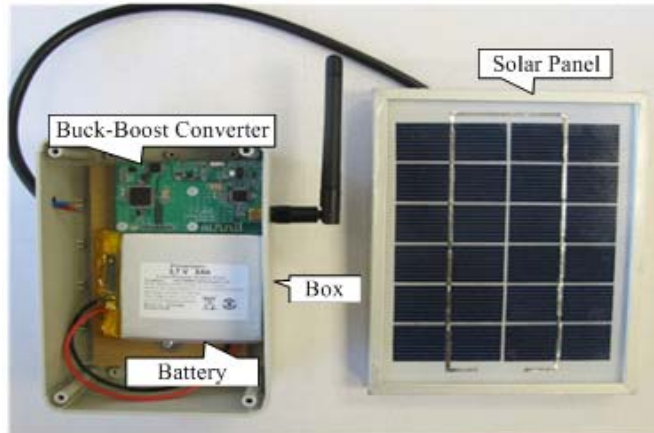
Fig. 7 Solar panel and Buck-Boost Converter   Fig. 8 The box for wireless sensor

- A box in Fig. 8 with battery, Buck-Boost Converter, wireless transmitter and acceleration sensor has been manufactured, and it will be installed in the bridge.

- Finish the design of a wireless accelerometer board. This board use CC2420 IC for wireless communication in Fig. 9. The CC2420 is a true single-chip 2.4 GHz IEEE 802.15.4 compliant RF transceiver designed for low-power and low-voltage wireless applications. It can provide an effective data rate of 250 kbps.
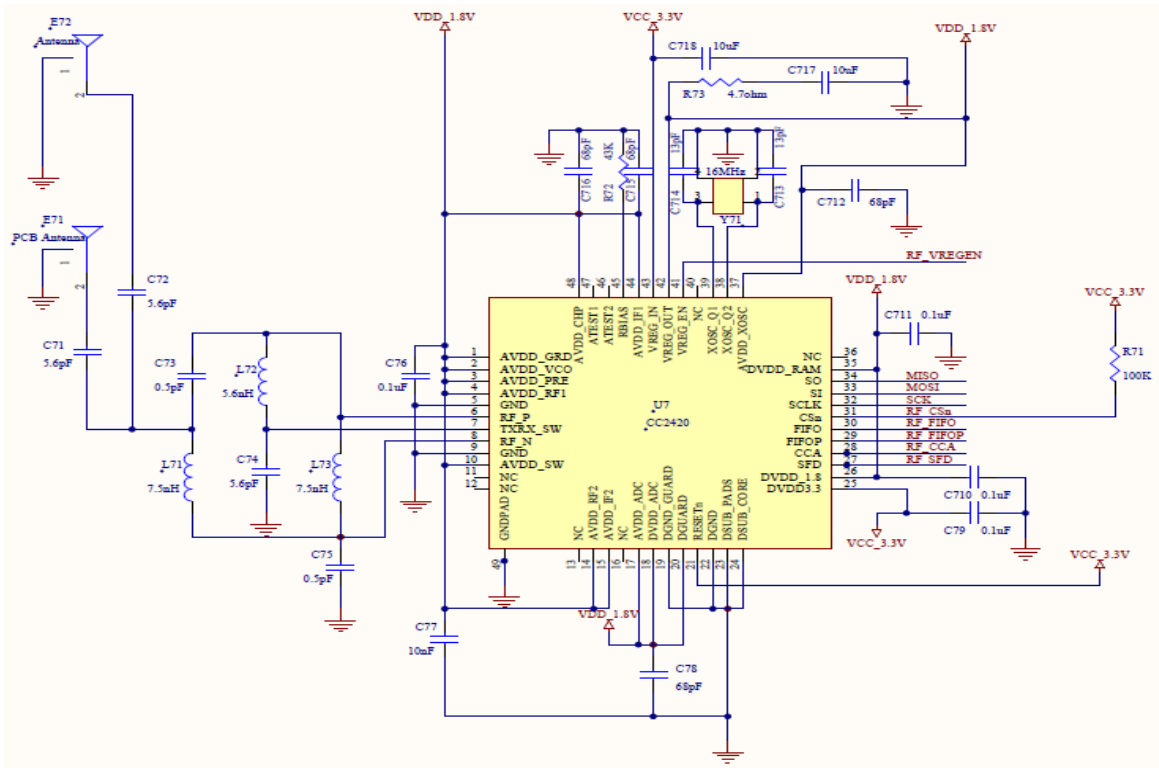
Fig. 9 The Schematic of CC2420

In Fig. 10, ATmega324P is for the micro controller unit on this board. It's a 8-bit AVR RISC-based microcontroller combines 32KB ISP flash memory with read-while-write capabilities, 1KB EEPROM, 2KB SRAM, 32 general purpose I/O lines, real time counter, three flexible timer/counters with compare modes and PWM, 2 USARTs, byte oriented 2-wire serial interface, 8-channel/10-bit A/D converter with optional differential input stage with programmable gain, programmable watchdog timer with internal oscillator, SPI serial port, JTAG (IEEE 1149.1 compliant) interface for on-chip debugging and programming, and six software selectable power saving modes. It can operate between 2.7-5.5 volts.
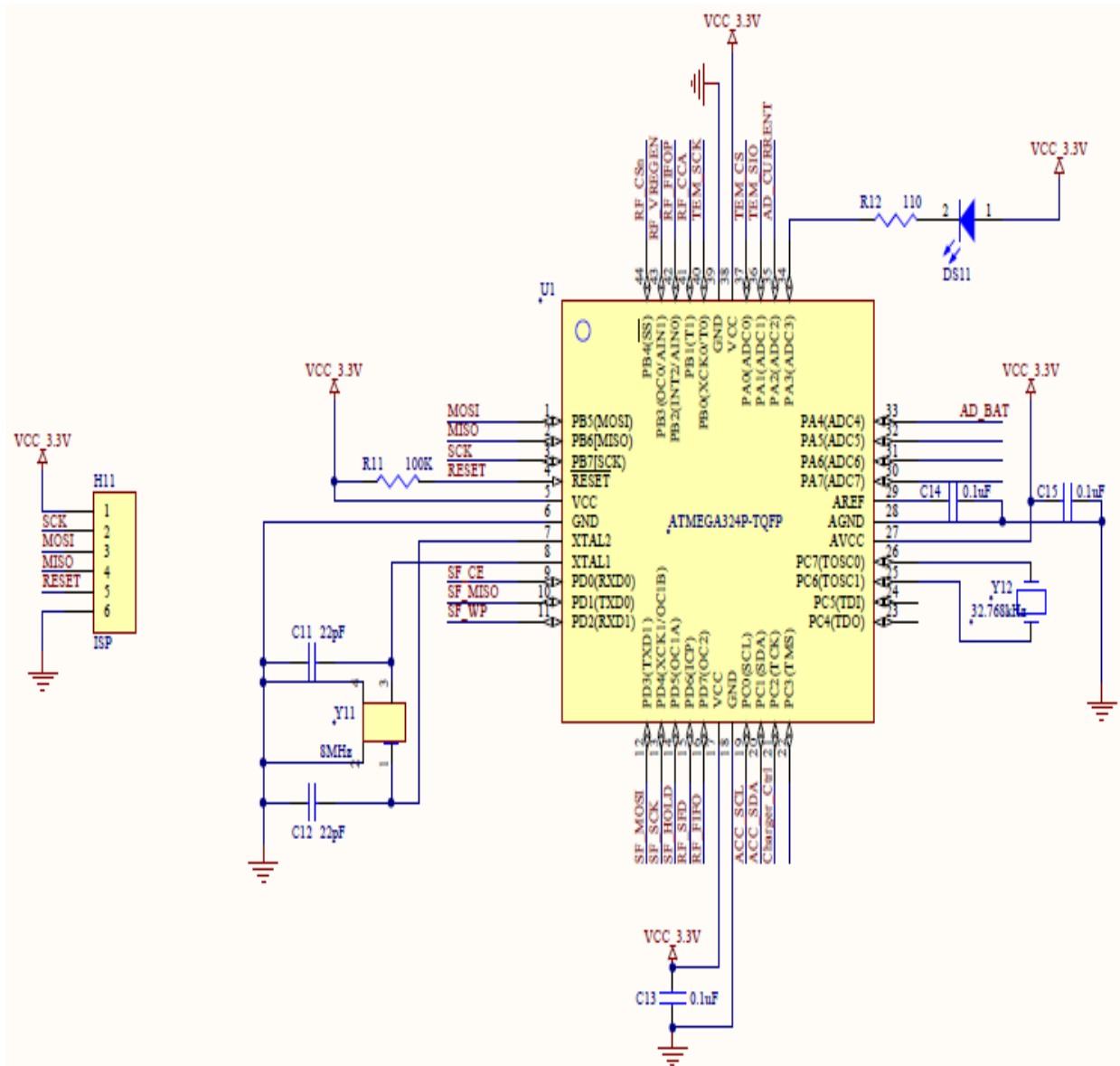

Fig. 10 The Schematic of ATmega324P

38

- Finished the PCB design and soldering work of the new wireless accelerometer board in Fig. 11 and Fig. 12.

Fig. 11 The PCB design of the new wireless accelerometer board

Fig. 12 The PCB board after soldering

- Designed the communication protocol of the new wireless accelerometer board. The program include five parts:
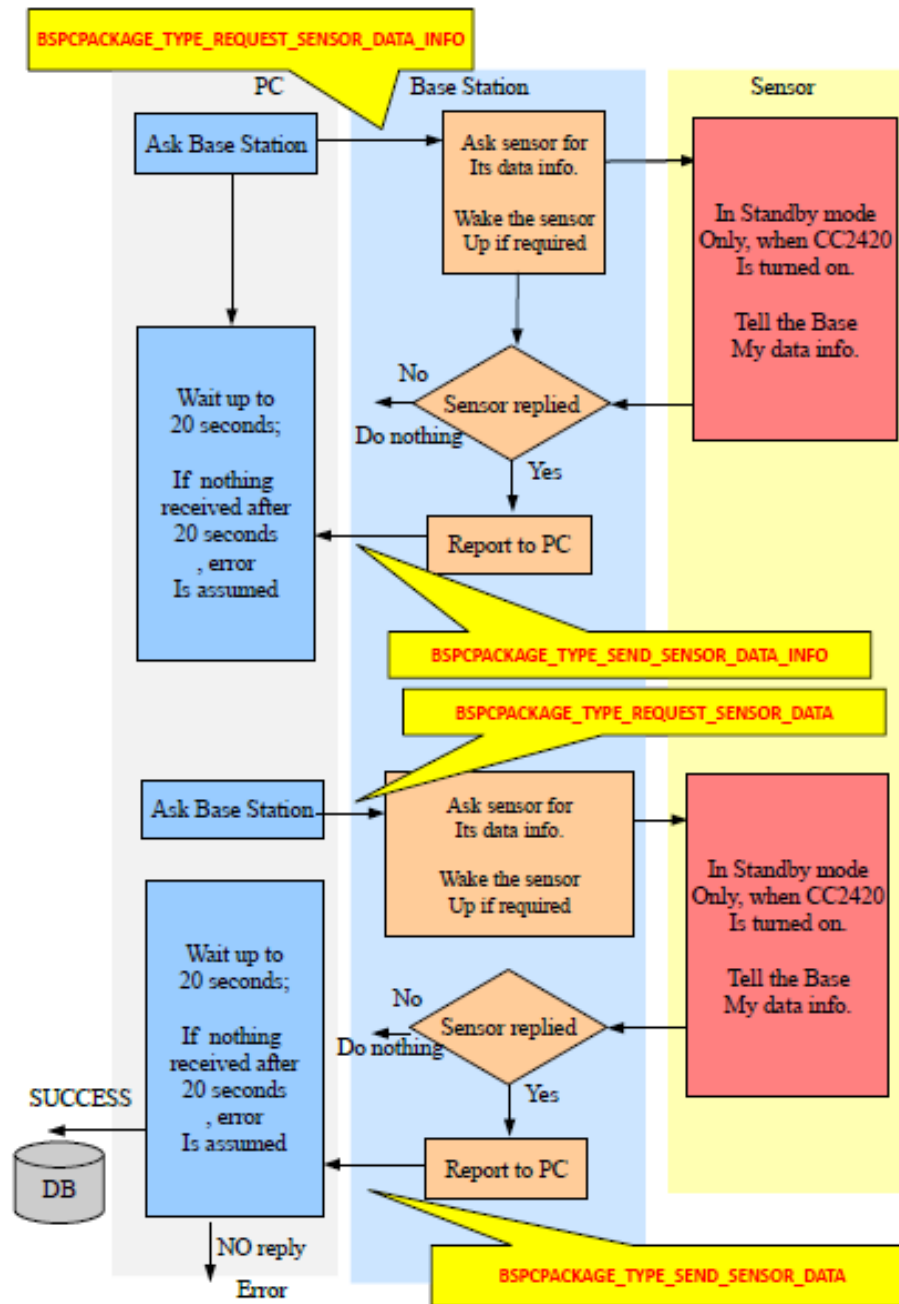
1. Automatically report network status;
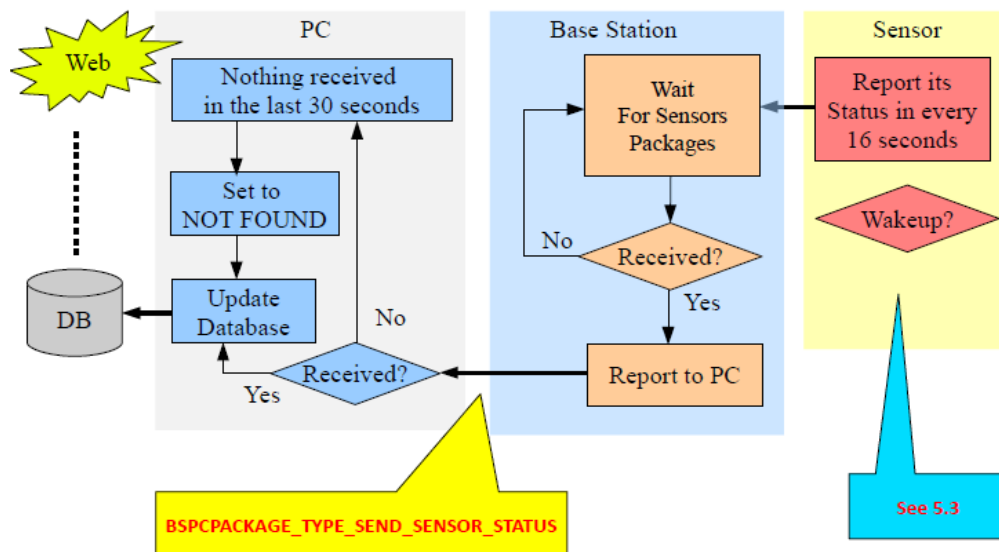
2. PC to Base Station Time Synchronization
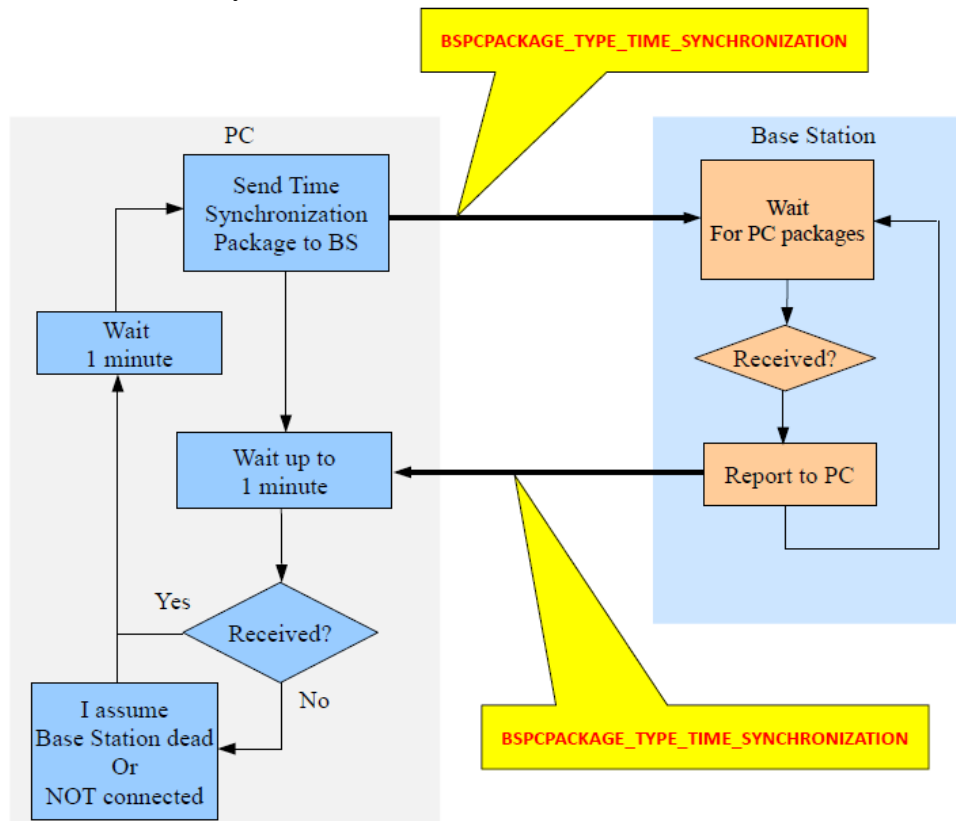
3. Data Acquisition Procedure.
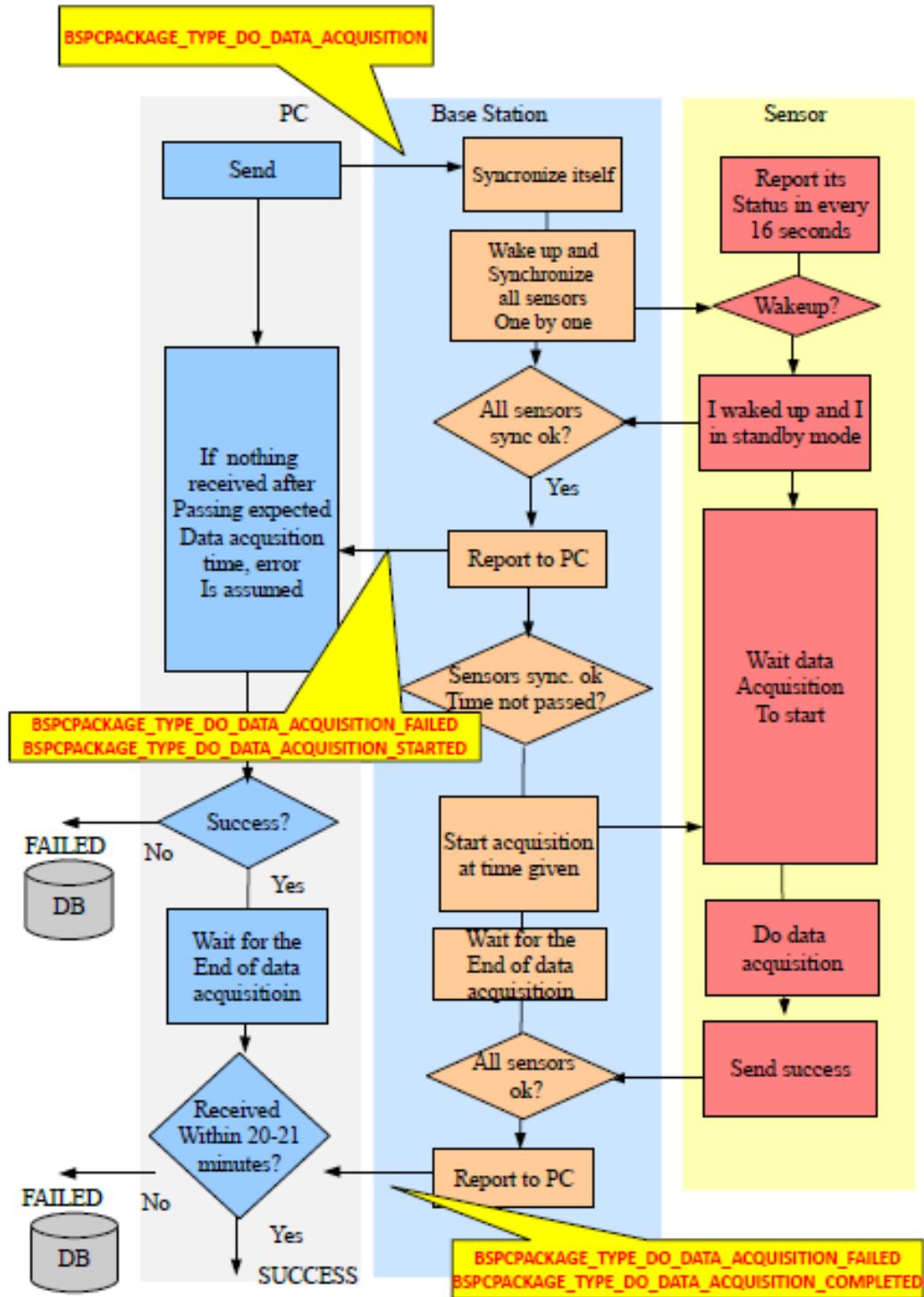
4. Retrieving Data Information and Data after successful data acquisition;

5.Launching sleep mode automatically: an auto-sleep function is implemented in the sensor firmware to put sensor back to sleep mode once there is no incoming radio activity for 1 minutes.